Vera Rute Soares Gomes

Licenciada em Conservação e Restauro

Effectiveness of aged graffiti cleaning technologies on cultural heritage granite

Dissertação para obtenção do Grau de Mestre em Ciências da Conservação

Especialização em pedra

Orientadora: Doutora Maria Amélia Alves Rangel Dionísio, Professora Auxiliar, IST-UL
Co-orientador: Doutor José Santiago Pozo-Antonio, Investigador, UVigo

FACULDADE DE CIÊNCIAS E TECNOLOGIA
UNIVERSIDADE NOVA DE LISBOA

Setembro 2017

Vera Rute Soares Gomes

Licenciada em Conservação e Restauro

Effectiveness of aged graffiti cleaning technologies on cultural heritage granite

Dissertação para obtenção do Grau de Mestre em
Conservação e Restauro

Especialização em pedra

Orientadora: Doutora Maria Amélia Alves Rangel Dionísio,
Professora Auxiliar, IST-UL
Co-orientador: Doutor José Santiago Pozo-Antonio, Investigador,
UVigo

FACULDADE DE
CIÊNCIAS E TECNOLOGIA
UNIVERSIDADE NOVA DE LISBOA

Setembro 2017

Acknowledgments

Resumo

Os graffitis, como resultado de atos de vandalismo, constituem uma das mais severas ameaças à pedra em Património Cultural. A sua limpeza é dispendiosa e pode acarretar danos físico-químicos. Os graffitis são muitas vezes executados em superfícies sem proteção anti graffiti e na prática são apenas removidos após longa exposição ambiental, levando à sua possível interação, seja com os agentes ambientais, seja com o substrato pétreo.

Esta dissertação pretende estudar até que ponto a exposição a ambientes contaminados vai influenciar a remoção dos graffitis, para assim fornecer elementos relevantes para futuras intervenções em Património Cultural.

Levaram-se a cabo dois conjuntos de estudos comparativos, em amostras não envelhecidas e em amostras artificialmente envelhecidas (em câmara climática com SO_2). Aplicaram-se quatro graffitis em aerossol sobre um granito da Península Ibérica, Rosa Porriño, que foram submetidos a diversos procedimentos de limpeza: dois métodos químicos, quatro métodos mecânicos e um laser.

Foram utilizadas técnicas de microscopia, métodos químicos e físicos para, em primeiro lugar caraterizar as tintas envelhecidas e não envelhecidas e posteriormente avaliar as performances de limpeza, tendo em conta o grau de extração de graffiti e efeitos nocivos.

Os resultados obtidos revelaram que o grau de limpeza com agentes químicos e laser está dependente da composição do ligante das tintas (resinas alquídicas ou de polietileno).

Importa também salientar o papel do SO_2 na performance dos vários métodos de limpeza. Após envelhecimento as tintas tornaram-se mais difíceis de limpar, apresentando maiores alterações globais de cor, maior percentagem de resíduos e superfícies mais hidrorrepelentes. As melhores performances de limpeza foram obtidas com o método químico baseado em hidróxido de potássio AGS 600® e com o mecânico Hydrogommage® com abrasivo à base de silício.

Por fim, apresentam-se algumas linhas de investigação futuras.

Palavras Chave: Património Cultural; granito; envelhecimento; tintas de graffiti métodos de limpeza; performance.

Encontra-se ainda um manuscrito aceite sob grande revisão à revista *Science of the Total Environment* e um manuscrito submetido à revista *Construction and Building Materials*.

Abstract

Graffiti paintings, as an act of vandalism, are one of the most severe threats to Cultural Heritage stone. The cleaning is expensive and may induce chemical and physical damages to the stone. Graffiti is often executed in surfaces without anti-graffiti protection and in real practice are only removed after long periods of environmental exposure, leading to their interaction with the environmental agents and with the stone substrate.

This dissertation intents to study to what extent the exposure to polluted environments will affect the graffiti removal, in order to provide relevant elements for future interventions in Cultural Heritage.

Two sets of comparative studies were conducted, on unaged and on artificially aged samples (in a climatic chamber with SO_2). Four graffiti aerosol paints were applied on an Iberian Peninsula granite, Rosa Porriño. Different cleaning procedures were applied: two chemical methods, four mechanical methods and a laser based-method.

Microscope techniques, chemical and physical analytic techniques were used in order to firstly asses the characterization of unaged and aged paints and secondly to evaluate the cleaning performances based on the graffiti extraction level and induced harmful effects.

The obtained results showed that the chemical and laser cleaning performance is associated to the binder composition of the paints (alkyd or polyethylene resins).

It must also be pointed out the role of SO_2 in the cleaning performance for all the cleaning methods. After ageing, the paints became more difficult to clean, presenting higher global colour changes, residue percentages and the surfaces became more water repellent. The best cleaning performances were achieved with the potassium hydroxide based chemical cleaner AGS 600® and the mechanical Hydrogommage® with silicon based abrasive.

Finally, some futures research lines are pointed out.

Keywords: Cultural Heritage; granite; ageing; graffiti aerosol paints; cleaning methods; performance.

List of Contents

List of Figures

List of Tables

1. Introduction

The term graffiti derives from the Italian word *graffiare* (to scratch) and can be defined as writing or drawings scribbled, scratched, drawn or painted, on a wide range of materials and substrates, mainly located in public accessible places, as result of a vandalism act [1]. Many cities worldwide spend huge amounts of money in cleaning campaigns to tackle graffiti vandalism [2]. The European Commission has financed projects with the aim to develop sustainable anti-graffiti products to ensure the satisfactory graffiti extraction without inducing damages on the substrate (GRAFFITAGE, 2005-2008) [2] and also focused on support urban environment policies to prevent and eliminate graffiti (GRAFFOLUTION, 2014-2016) [3].

However, in many cases, graffiti is done in historic surfaces without anti-graffiti protective coatings and in real practice, they are not shortly removed after their execution, i.e., most of the times they are cleaned after long term environmental exposure. This leads the graffiti to interact with the environmental agents (e.g. rain and atmospheric pollutants) and with the stone substrate. Along with the previously mentioned consequences it must be added the damages associated to cleaning, such as surface abrasion, chemical contamination or mineralogical alterations [4,5]. There are different cleaning methods, being the most traditional the chemical and mechanical. Most scientific production focuses on graffiti cleaning of carbonate stones [6] (Appendix 7.1). In the last decade, the application of the laser to clean Cultural Heritage stone has been investigated [6].

To the best of our knowledge, there are no scientific studies focused on aged graffiti removal. Therefore, this research aims to firstly characterize the ageing process of graffiti paints and to optimize their removal from a granite subjected to SO_2 rich atmosphere through different cleaning procedures: chemical, mechanical and laser.

2. State of the art

An evaluation of the graffiti aerosol paints and their removal methods, considering the stone type, the paints binder composition and the removal method is here briefly presented. More details can be found in [6].

2.1. Graffiti aerosol paints

The range of materials used by graffiti-writers is fairly extent and can often be found in multiple layers, superimposed, requiring a sequence of methods/products to be removed [7,8]. Aerosol paint outlines as the main material used by graffiti-writers due to its visual impact and quick and easy application [5,9]; they are composed of pigments that provide colour and opacity, additives that improve certain properties (e.g. plasticity, fluidity, thickness, etc.), a solvent that allows this mixture to flow and a binder that holds this mixture together to the substrate [10].

These paints may harden by evaporation of the solvent or through polymerization [1]. The paints that harden by evaporation of the solvent can be dissolved through re-application of the solvent to return to the previously liquid state [1,7]. The paint may penetrate to various depths depending on factors like a high solvent content (that implies a higher flow rate), the interfacial tension solid surface/liquid and the substrata characteristics [10]. Is barely impossible to distinguish the type of paint without proper analysis and most of the times on-site trials are used to decide the most suitable cleaning method [1].

From the universe of graffiti aerosol paints covered by the literature, it is important to highlight some brands that were specially developed for the graffiter's market such as Montana Colours®, Felton®, Krink® and Nero D'inferno® [6].

White pigments are the main component of all paints (white and coloured); titanium confers whiteness, brightness and opacity to graffiti in Montana Colours® [11–14], Trans-colour® [15,16], Felton® [15,16] and Motip-Dupli®. Black colour is often obtained by adding carbon, silver colour by aluminium and gold colour by zinc and copper (Montana Colours® in [11–14]) and (Trans-colour® in [15,16]).

Additives may be also present in small amounts: plasticizers or dispersants to increase plasticity or fluidity, surfactants and wetting agents to disperse pigments, thickeners, pH buffers to stabilize the pH range, anti-foaming agents to alter the surface tension of a paint, freeze–thaw agents, biocides and sequestering agents to remove metal ions [5,9]. The main synthetic binders in twentieth-century paints are acrylic, alkydic and nitrocellulosic [17].

Acrylic resins are based on the esters of acrylic and methacrylic acids [17] and can be found in Krink® and Nero D'inferno® cutting edge paints [18,19]. This paint may be purely acrylic or copolymerized with other vinyl species, such as styrene which is present in low-cost paints and also in artist quality paints, like Trans-colour® and Felton® [15,16].

Alkydic resins are polyesters formed by a polyalcohol and a dicarboxylic acid [17]. Its drying mechanism is similar to oil paint, i.e. complex oxidative polymerization reactions resulting in a cross-linked insoluble film [17]. These resins were identified in Motip-Dupli® Montana Black [20], Montana Colours® [11–14] and Motip Home & Hobbylacquer® [10,21,22].

Nitrocellulosic resins are composed of cellulose nitrate, a second resin (usually alkydic) and large quantities of plasticizers (mainly dibutyl and dioctyl phthalate). It is formulated as a solution that can be re-dissolved in the same solvent [17]. Almost half of 51 red aerosol paints analysed by Govaert & Bernard, were composed of alkyd-nitrocellulose-based binders [23]. Samolik *et al.* also detected in Motip-Dupli® Montana Gold an acrylic resin along with nitrocellulose [20].

The main aerosol paint solvents are hydrocarbons (aliphatic, naphthenic and aromatic-toluene and xylene), oxygenated (ketones, esters, glycol esters and alcohols-especially n-butanol) and water [5,9].

2.2.   Graffiti removal methods

Graffiti removal procedures, despite apparently simple, are potentially harmful and basically irreversible interventions. Several recommendations for the cleaning of Cultural Heritage stone have been proposed in the past decades [24,25] as well as methods for assessment the cleaning results [26]. In addition to it, must also be considered the chemical composition of the paint and the intrinsic properties of the stone. Most of the scientific production focus graffiti cleaning of carbonate stones (Appendix 7.1), namely limestone and marble. The traditional removal procedures applied by professionals are the chemical and mechanical based methods, probably because they are the most economical methods. Nevertheless, scientific publications based on the evaluation of their cleaning effectiveness are scarce, being the publications led by the laser studies (Appendix 7.1).

2.2.1.   Chemical removal methods

Chemical cleaning is due to the reaction between the chemical remover and the paint, achieving its dissolution and extraction [27]. Chemical agents are available in various compositions and consistencies (e.g. gels and poultices) to be adapted to different substrates [1,28]. Already in 1999, Urquhart reported the ghosting due to graffiti penetration, mainly in porous stones [7], later corroborated by other authors [18,19].

The traditional solvents recommended for limestone, marble, sandstone, slate and granite are usually based on organic solvents like methylene and acetone or alkali caustic removers [29]. These organic solvent based removers work by weakening the adhesion between the paint and the stone, while caustic removers broke down alkydic based paints by saponification [1,7]. In Avebury Neolithic sandstones and Stonehenge Heel a combination of methylene dichloride and acetone (prior to laser application), was successfully tested to remove the remaining paint [30]. More recently Samolik *et al.* used a mixture of ethanol, acetone and xylene to successfully remove nitrocellulosic acrylic and alkydic based paint (Montana Gold from Motip-Dupli®) on limestone, sandstone, plaster and brick. However, they did not succeed in removing the alkydic black paint Montana Black from Motip-Dupli® [20]. Carvalhão & Dionísio used a solution based on potassium hydroxide (AGS 60^{TM}) to remove Motip Home & Hobbylacquer® paints and achieved a homogeneous cleaning on Branco marble, while for Lioz limestone an extra-accumulation on stilolytes was registered [21]. The surface lightness also increased and dissolution of grain boundaries and loss of crystals was detected. Pozo-Antonio *et al.* tested Wendrox® and Eligraf® (based in organic solvents) and QuitaGraffi 200®– QuitaSombras 60® (QG+QS) rich in potassium hydroxide on two granites (Silvestre and Rosa Porriño), with satisfactory results for various alkydic Montana Colours®. The silver graffiti

required a subsequently application of TS-99 paint stripper [13]. Chemical contamination was also detected with Wendrox® and QG+QS.

2.2.2. Mechanical removal methods

The mechanical cleaning acts through an abrasive process of the surface and is frequently associated with an heterogeneous cleaning, damage and an increase of the susceptibility to retain soiling by the substrate [1,28]. The pressure applied may have an abrasive effect and cause damage as verified by various authors in dolomitic marble [18,19] and on limestone, sandstone, plaster and brick with high-pressure water jet and blast cleaning [20]. Recently, Careddu & Akkoyun studied the best water-jet cleaning operational conditions for Carrara marble, finding the best results with an inter-distance between passes of 0.5 mm, 200 MPa water pressure, 12.0 mmin^{-1} travel speed [31].

In the last years, low pressure projection methods have been developed with the aim to reduce the substrate damage. Low pressure steam was used to remove a water soluble white paint from Avebury Neolithic Sandstone [30]. Carvalhão & Dionísio tested Sponge-Jet® (a blasting media with a sponge-like urethane polymer involving spherical calcium carbonate particles) and Exastrip® (pure spherical calcium carbonate particles) at low pressure (0.5–2.5 bar) to clean Branco marble and Lioz limestone [21]. Despite their successful cleaning level, punctual paint traces were found in Lioz stilolytes. The topography changes were reduced comparatively to those registered on the surface cleaned with an alkaline cleaner. However the hydrophobicity increased, probably due to unremoved polymers and also significant global colour changes were detected. Pozo-Antonio *et al.* tested Hydrogommage®, based on the circular projection of air–water–micro grained abrasive (99% SiO_2 content, 0.5–0.1 mm grain size mixture) at low-pressure (0.5–1.5 bar) to clean various Montana Colours® alkydic aerosol paints on Rosa Porriño and Silvestre granites with satisfactory results. However, an increase around 10 μm on the average roughness for both substrates was reported [13]. In a later work [32], the same authors used hyperspectral imageing technique to characterize the cleaning performances, being Hydrogommage® and the nanosecond-pulsed Nd:YVO$_4$ laser working at 355 nm the more suitable techniques.

2.2.3. Laser removal methods

The mechanism responsible for laser cleaning is the ablation; the undesired layers are removed by the beam irradiation when the fluence (energy deposited per unit area) exceeds its critical extraction threshold [33,34]. The most used lasers are neodymium-based systems, i.e. Nd:YAG or Nd:YVO$_4$ [4]. Laser allows non-mechanical contact, has a selective action since it provides a located and accurate cleaning and adjustment in real time [4]. In 2003, Costela *et al.*

were the pioneers to apply this technology to remove paints on marble obtaining satisfactory results without damage using a Nd:YAG at 355 nm (3rd harmonic) whereas at 532 nm (2nd harmonic) left residues of polymeric base [15]. Later Gómez *et al.* used the same paints and stone to compare Nd:YAG working at the fundamental harmonic 1064 nm with XeCl excimer at 308 nm. While Nd:YAG left residues and darkened the surface, XeCl achieved satisfactory results without damage [16]. Daurelio working at 1064 nm and 532 nm tested three laser protocols for graffiti removal on Bisceglie dolmen with a Nd:YAG [35]: 1) A laser beam in air or via a guiding fibre glass, removed satisfactorily black paint; 2) A rectangular-shaped laser beam removed ink, graphite and aerosol paints; and 3) A rectangular-shaped laser beam with a mixture of water and red-brown earth removed paint markers. Later, Andriani *et al.* successfully removed inks with the third protocol and with the second one with water [36]. Ortiz *et al.* cleaned different paints on dolomitic white marble with Nd:YAG laser working at 266 nm. At 1064 nm it was only achieved the removal of black aerosol but with yellowing effect [19]. Samolik *et al.* also reported yellowing with 1064 nm, darkening with 355 nm and satisfactory results with 532 nm [20]. While MotipDupli® Montana Black paints were not successfully removed, satisfactory results were obtained for MotipDupli® Montana Gold [20].

Fiorucci *et al.* studied different fluence values (from 0.1 J cm^{-2} to 1.2 J cm^{-2}) of Nd:YVO$_4$ laser at 355 nm applied on Rosa Porriño granite finding optimal results with 0.1 J cm^{-2}. Undesirable damages, such as melting of the biotite and loss of the pink colouration of the K-feldspar grains occurred in cleanings at 0.3 Jcm^{-2} [11]. Other researchers concluded that Fe compounds are very sensitive in response to 1064 nm laser irradiation [37,38]. Urones-Garrote *et al.* tested Nd:YAG at 355 nm and assigned the decolouration effect of the pinkish Rosa Porriño granite to the induced thermal effects in the microstructure and composition of potassium feldspar grains [39]. Rivas *et al.* working with Nd:YVO$_4$ at 355 nm to clean several graffiti on Vilachán and Rosa Porriño granites confirmed the influence of the chemical composition of the graffiti paint on the cleaning effectiveness. The cleaning of red, blue and black paints from Montana Colours® had similar satisfactory results, while silver graffiti displayed a translucid film [14]. Paint penetration into the granite fissures was reported and remained after cleaning. Laser also caused melting of the biotite grains, fracturing of the quartz grains and a possible change in hydration of iron oxides and oxyhydroxides covering fissures was found. Pozo-Antonio *et al.* also applied the same laser and paints on Silvestre and Rosa Porriño granites [13]. The laser was satisfactory for all the paints except silver graffiti. In fact, in the surface cleaned of silver graffiti, a carbon and aluminium film was detected by SEM. Despite these results for the silver paint, in a later study [32], the laser proved by means of hyperspectral imageing technique to be one of the most suitable cleaning techniques. More recently Ramil *et al.* studied the optimal laser fluence ranges to clean graffiti paints on silicates with the previously used laser and paints on Rosa Porriño granite [39]. The cleaning effectiveness was found to be

influenced by the polymineralic characteristics of the granite since the four main minerals presented different behaviours. For quartz and K-feldspar grains the higher cleaning effectiveness levels were achieved with 0.1–0.2 Jcm^{-2} for all colours; for plagioclase, was achieved from 0.1 to 1.0 Jcm^{-2} depending on the graffiti colour and biotite started to be cleaned with 0.06 Jcm^{-1} (with melting occurrence at the lowest fluence). Textural characteristics of the stone such as fissural system and cleavage also interfere in the graffiti penetration and the cleaning performance [40].

3. Materials and methods

3.1. Stone material

A granite, Rosa Porriño, was selected from northwest Iberian Peninsula. It is a two-mica calcoalkaline coarse-grained granite with a panallotriomorphic heterogranular texture. Two hundred and forty samples with 1.5 cm thickness, measuring 5 cm x 5 cm were prepared from commercial disc-cutting finished-slabs. More information regarding this stone can be found in (Appendix 7.2).

3.2. Aerosol paints

Four colours of graffiti aerosol paint from Montana Colours® were selected based on previous researches [11,12,14,41] due to their different responses to conventional cleaning procedures: devil red (R-3027), ultramarine blue (R-5002), graphite black (R-9011) and silver chrome (RAL-7001). The paints were sprayed at an angle of 45° and from a distance of 30 cm over the disc-cutting face of the samples to facilitate identification of surface alterations after SO$_2$ exposure. The paints were also applied on microscope slides (three slides per colour). The painted samples were left to air-dry in the laboratory (18±5ºC; 60±10% HR) for seven days.

3.3. SO$_2$ artificial ageing

After the aerosol paints properly dried on stone surface, half of the samples were kept during two months in the laboratory under room conditions (18±5ºC; 60±10% RH) hereinafter designated as unaged, while the other half was placed during two months in a climatic chamber (FITOCLIMA 300EDTU) with SO$_2$ artificial ageing at (25ºC and 98% RH) hereinafter designated as aged. Moreover, microscope slides painted with each graffiti colour were also subjected to the same procedure. The stablished RH value was used to simulate a frequently occurring outdoor condition, where stones are coated with a thin film of condensed moisture [42]. It has been pointed out that a high RH accelerates sulphate attack by SO$_2$ dry deposition [43,44]. The SO$_2$ contaminant (SO$_2$ diluted at 3% in 3000 ppm of nitrogen) was dosed at a concentration of

200 ppm, which is about 4000 times higher than current SO_2 levels in most urban areas from Europe [44–46]. It was decided to use this high concentration to obtain a high reaction rate.

3.4.   Cleaning methods

The unaged and artificially aged samples were cleaned with different procedures, namely: two commercial chemical products, two mechanical methods with two abrasives each and a laser method.

In what concerns the chemical methods two different commercial products were used:

- A solution of potassium hydroxide (10–30% wt%) with surfactants (2-aminoethanol, 1–2% wt%), from Trion Tensid AB, Sweden (AGS 600®), hereinafter designated as **AGS**;

- A solution of n-butyl acetate, xylene and alcohol isobutyl, from 3M, Spain (Graffiti GR3®), hereinafter designated as **GR3**.

These commercial chemical products were applied over stone surfaces with a soft brush and following suppliers' recommendations *AGS* was left to act for 10 minutes and *GR3* for 2 minutes. After this time, the graffiti paints were removed by energetic brushing with hot tap water rinse (50°C) and with natural tap water rinse respectively. This procedure was repeated until a satisfactory cleaning was achieved, with a maximum of 5 cleaner applications and it was interrupted when the operator felt that more repetitions would not improve the final result. Afterwards the samples were left to dry for 15 days at laboratorial room conditions (18±5ºC; 60±10% HR). The pH measurements of *AGS* showed that is a highly alkaline product with values above 14.

Regarding the mechanical methods two different commercial equipment's were used:

- An equipment based on the circular projection of a mixture of air, water and micro abrasive (Hydrogommage®). Two sharp edged abrasives were used: silicon and aluminium silicate, both at pressure of 2 bars. Silicon abrasive is composed according to the technical sheet, around 98.6% SiO_2, with almost 90% of particles comprised between 75-106 µm grain size (Appendix 7.3). Aluminium silicate abrasive is composed of 45-52% SiO_2 and 24-31% Al_2O_3 and presented a coarser grain size of 160-80 µm according to the technical sheet (Appendix 7.3). Hereinafter designated as **Hydro Si** and **Hydro Si Al** respectively.

- An equipment based on the circular projection of air and micro grained abrasive (IBIX®). Two abrasives were tested at pressure of 4 bars: the previously reported silicon and round shaped microparticles of $CaCO_3$ with around 98% of $CaCO_3$ and grain size comprised between 70–200 µm according to the technical sheet (Appendix 7.3). Hereinafter designated as **IBIX Si** and **IBIX Ca** respectively.

After the mechanical cleanings, the residues (abrasive and graffiti paints) were removed by tap water rinse. The FESEM characterization of the micro abrasives (Appendix 7.4) confirmed their composition, dimensions and morphology.

Lastly a laser method was tested:

- A Nd:YVO$_4$ Coherent AVIA Ultra 355–2000® laser at the 355 nm wavelength and with 25 ns pulse duration (Appendix 7.5). The frequency (10 000 Hz), fluence (0.1-0.3 J.cm^2), scan speed (25 mm.s^{-1}), distance between scans (0.075 mm) and laser trajectory parameters (horizontally and vertically alternated with no more than four scans) were selected on the basis of previous studies in granites [11–14,40] and preliminary cleaning tests evaluated under a stereomicroscope.

3.5. Analytical techniques

In figure 3.1 is presented the experimental design of the laboratorial procedures used in the different phases of the study, namely the characterization of the (unaged and aged) aerosol paints and the cleaning methods performance. In the following sections, a brief description of each phase will be presented.
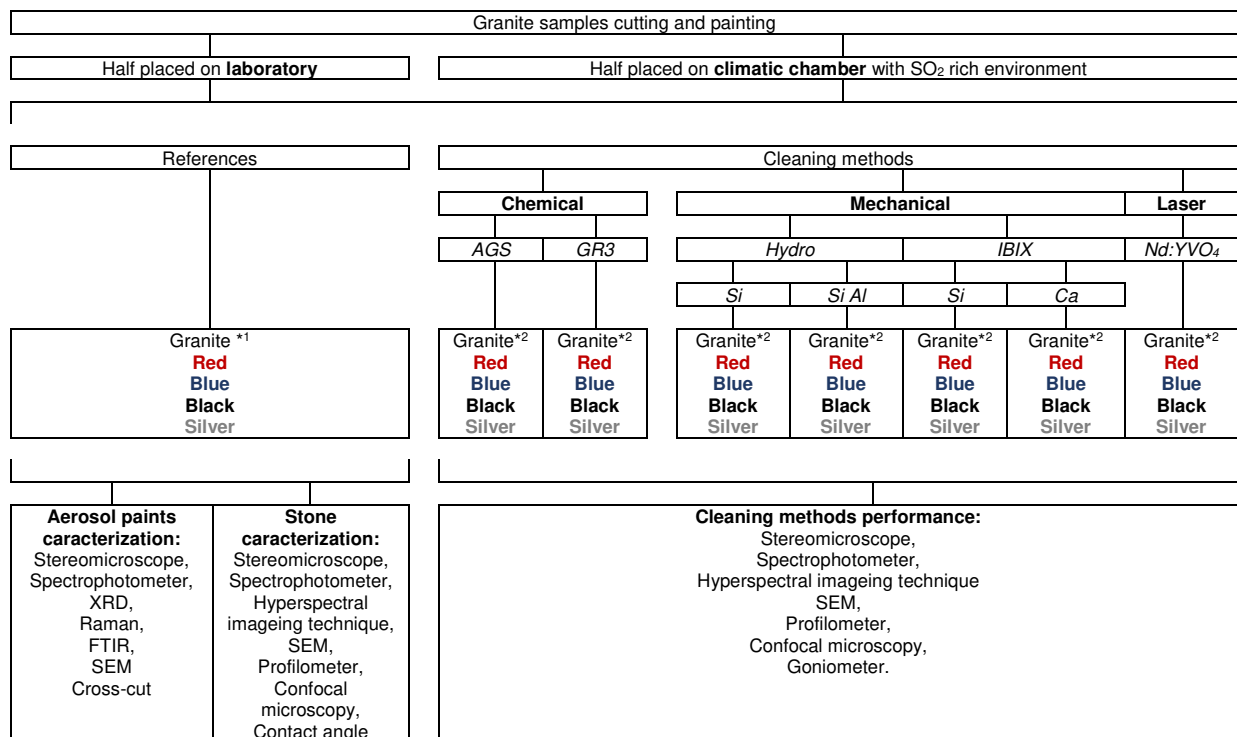
Fig.3.1 – Experimental design of the laboratorial procedures for the characterization of the paints, stone and cleaning methods performance. *1 refers to the stone reference, *2 refers to the stone submitted to the several cleaning methods.

3.5.1. Aerosol paints characterization

In order to find any possible changes in the formulation of the aerosol paints by the manufacturer since the previous characterizations [10,13] and also to identify any morphological, chemical and mineralogical changes due to the artificial ageing, painted microscope slides and painted stones subjected to SO_2 were evaluated and the results were compared with those obtained for the unaged samples.

A first evaluation of the stones subjected to SO_2 was performed by means of a stereomicroscope (Nikon Eclipse 800).

Then, in order to identify chemical and mineralogical changes in the aerosol graffiti paint, the painted microscope slides were evaluated through X-ray fluorescence (XRF), X-ray diffraction (XRD), Raman spectroscopy and Fourier transform infrared spectroscopy (FTIR) (Appendix 7.6). Chemical changes were characterized by XRF (ArtTAX, 800 spectrometer). Mineralogical changes were identified by XRD with a diffractometer (XPERT-PRO) by the random powder (grazing incidence) method. Raman spectroscopy was used to study the nature of the crystals developed over the aged silver paint (LabRam HR Evolution spectrometer). The aerosol paints functional groups were evaluated by FTIR using a Nicolet 6700 with a DTGS KBr detector.

Gold-palladium coated samples of the painted stones surfaces were evaluated to find any physical or chemical alterations and formation of sub-products using two scanning electron microscopes with energy-dispersive x-ray spectroscopy (SEM-EDS) (Philips XL30 and JEOL JSM-6700) in Secondary Electrons (SE) and Back Scattered Electrons (BSE) modes.

The colour changes of the surfaces of the painted samples after SO_2 exposure were quantified with a spectrophotometer (Minolta CM-700d) in the CIELAB colour space (Appendix 7.6). A total of 20 measurements for each sample were made, being each an average of 3 measurements (as recommended by Prieto *et al.* for a granite with this grain size [47]). The chroma, colour purity C*$_{ab}$ was calculated based on a* and b* values, as follows: $C_{ab}^* = (a^{*2} + b^{*2})^{1/2}$ and for the colour difference the equation $\Delta E^*_{Lab} = \sqrt{(\Delta L^*)^2 + (\Delta a^*)^2 + (\Delta b^*)^2}$ [48], was considered, being each Δ the difference between the reference (unaged paint) value and after the ageing process.

The adhesion of the paints was evaluated by Cross-Cut-Test [49]. A total of 6 grid lines in each sample surface were performed with a cross hatch cutter (Elcometer 107) with cutter blade 1, followed by adhesive tape application and removal in 180º after 5 minutes of contact. The paint detachment was assessed by stereo microscopy and classified from 0-5, best to worst according to UNE-EN-ISO-2409 [49]. The statistic hypothesis t-student test was used to statistically validate the obtained data.

3.5.2. Cleaning evaluation

The performance of the cleaning methods was evaluated based on the graffiti extraction level and harmful effects (physical, chemical or mineralogical induced alterations).

Firstly, the cleaned surfaces were observed with the previously referred stereomicroscope and SEM.

The parameters of CIELAB space were measured and the global colour change ΔE_{Lab} was computed. The residual staining (RS) after the cleaning procedures was also evaluated using the formula proposed by Masieri & Lettieri: $RS = [(\Delta E^*_{ab})c/(\Delta E^*_{ab})s] \times 100$ where $(\Delta E^*_{ab})c$ and $(\Delta E^*_{ab})s$ correspond respectively to the colour variations of the cleaned and painted surfaces versus the granite reference [50], being each Δ the difference between the reference (before graffiti application) value and after each cleaning method.

Hyperspectral imageing technique was used to study the reflectance changes of the surfaces after the cleaning. The system consisted in a CCD sensor Pulnix TM-1327 GE with an objective lens, focal 10 mm and a spectrograph ImSpector V10 with 4.55 nm resolution (Appendix 7.6). Three measurements per sample were performed. The Least square based orthogonal subspace (LSOSP) method [40,51] was used to determine the coefficient of abundance α since the higher α, the cleaner the surface should be. In this abundance, a dominant signal (granite) was assumed. Other signals from the paint were undesirable interferences that must be eliminated to improve the detectability of the dominant signal. For this, an orthogonal projector to the subspace of the undesirable signals was developed: $P = I - UU^{\#}$, being I: identity matrix (L x L, L is the number of channels of the spectrum), U is the matrix with the signals to be removed and $U^{\#} = (U^T U)^{-1} U^T$. Then, the coefficient of abundance α using LSOSP was calculated as: $\alpha_{LSOSP} = (d^T P\, d)^{-1} d^T P\, r$, where d is the matrix of the stone spectrum and r is the matrix composed with cleaned surface. Then the higher the α_{LSOSP} the more satisfactory the cleaning performed.

The roughness of the surface was measured with a profilometer (Surfecoder SE1200). A scan length of 4 mm and 10 scans per sample was considered. The arithmetic average roughness (Ra) was measured. The statistic hypothesis t-student test was used to statistically validate the obtained roughness data. Moreover, in order to establish the extent of the topographical variations that could be accepted has a result of a cleaning procedure, the methodology proposed by Gaspar *et al.* was adopted to Ra parameter [52]. The damage threshold was calculated by adding to the stone reference Ra the respective standard deviation, and then comparing the obtained value with the Ra's after the diverse cleaning treatments. The values obtained above this damage threshold are statistically attributed to the impact of the cleaning procedures.

Confocal microscopy allowed to obtain a 3D surface roughness image (CM; PLu 2300 Sensofar® optical imageing profiler). Three images per samples were collected with an EPI 10X-N objective, an overlapping of 25%, a depth and a lateral resolution of 6.05 mm and 4.54 mm respectively. The acquired data were processed with Gwyddion software.

In order to verify if surface hydrophobe alterations occurred, static contact angles were measured with a goniometer (CAM 100, KSV, Helsinki, Finland) equipped with a digital camera and image analysis software. A total of 5 measurements per sample were made, at room temperature (20°C) by applying the sessile drop method. Deionized water was used as the wetting liquid with a droplet volume of 13 μL.

4. Results and discussion

4.1. Aerosol paints characterization

The red, blue and black graffiti paints after being submitted to a SO_2 rich environment did macroscopically not presented any signs of degradation (Fig.4.1 A, D and G). The silver paint, however, showed graffiti losses and formation of crystals (Fig.4.1 J). Contrary to the other paints inside the climatic chamber, silver graffiti was coated with water drops.
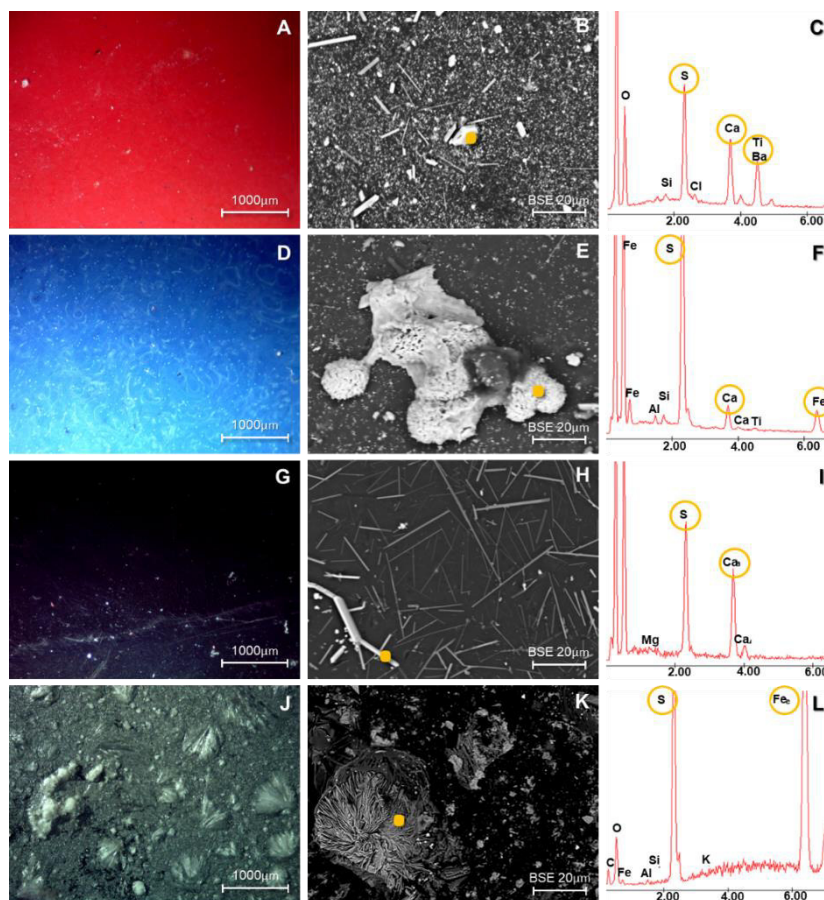
Fig.4.1 – Stereomicroscopy and SEM-micrographs of the aged paints (after SO_2). Moreover, EDS spectra of the neoformed structures are provided. A-C: Red paint. D-F: Blue paint. G-I: Black paint. J-L: Silver paint.

11

Concerning the chemical composition, XRF spectra (Fig.4.2) showed common elements for all paints: K, Ca, Ti and Fe; moreover, red and blue paints (Fig.4.2 A and B) also present Cl, blue and black paints (Fig.4.2 B and C) contain Co and Cu and silver paint present Al (Fig.4.2 D). It must be noticed that are two peaks in all XRF spectra, the inelastic (or Compton) diffusion around 16.4 keV and the peak corresponding to the molybdenum (Mo) equipment ampoule around 17.3 keV. The identified elements confirm the previous studies [11,14]. The emergence of sulfur Kα assignment was noticed in all paints after the artificial ageing.
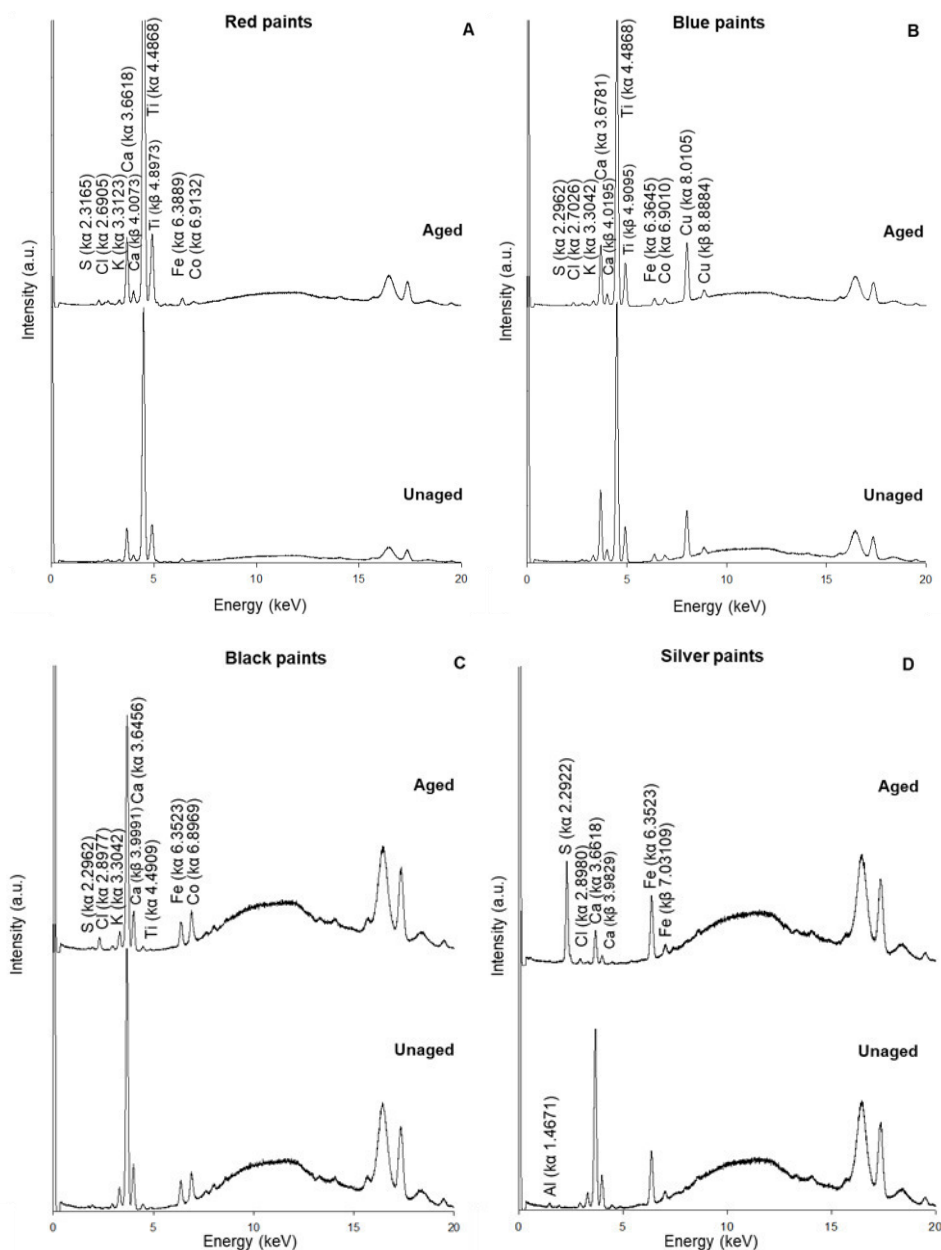
Fig.4.2 - XRF spectra of aged and unaged red (A), blue (B), black (C) and silver (D) paints.

XRD on the unaged paints allowed to identify titania (TiO_2) in red and blue paints (Fig.4.3 A and B), barite ($BaSO_4$) in red paint and aluminium (Al) in silver paint (Fig.4.3 D), corroborating the results of previous characterizations [11,14]. In Appendix 7.7 is presented the XRD peak list

of the three more intense peaks for each identified aerosol paint. Aluminium has also been reported in previous studies with Trans-colour® silver aerosol paints [15,16]. Diffractograms of the artificially aged paints showed the presence of gypsum ($CaSO_4 \bullet 2H_2O$) on both red and black paints (Fig.4.3 A and C) and alunogen ($Al_2(SO_4)_3 \bullet 16H_2O$) and metalunogen ($Al_2(SO_4)_3 \bullet 12H_2O$) on silver paint (Fig.4.3 D). Raman spectroscopy confirmed the presence of alunogen in the
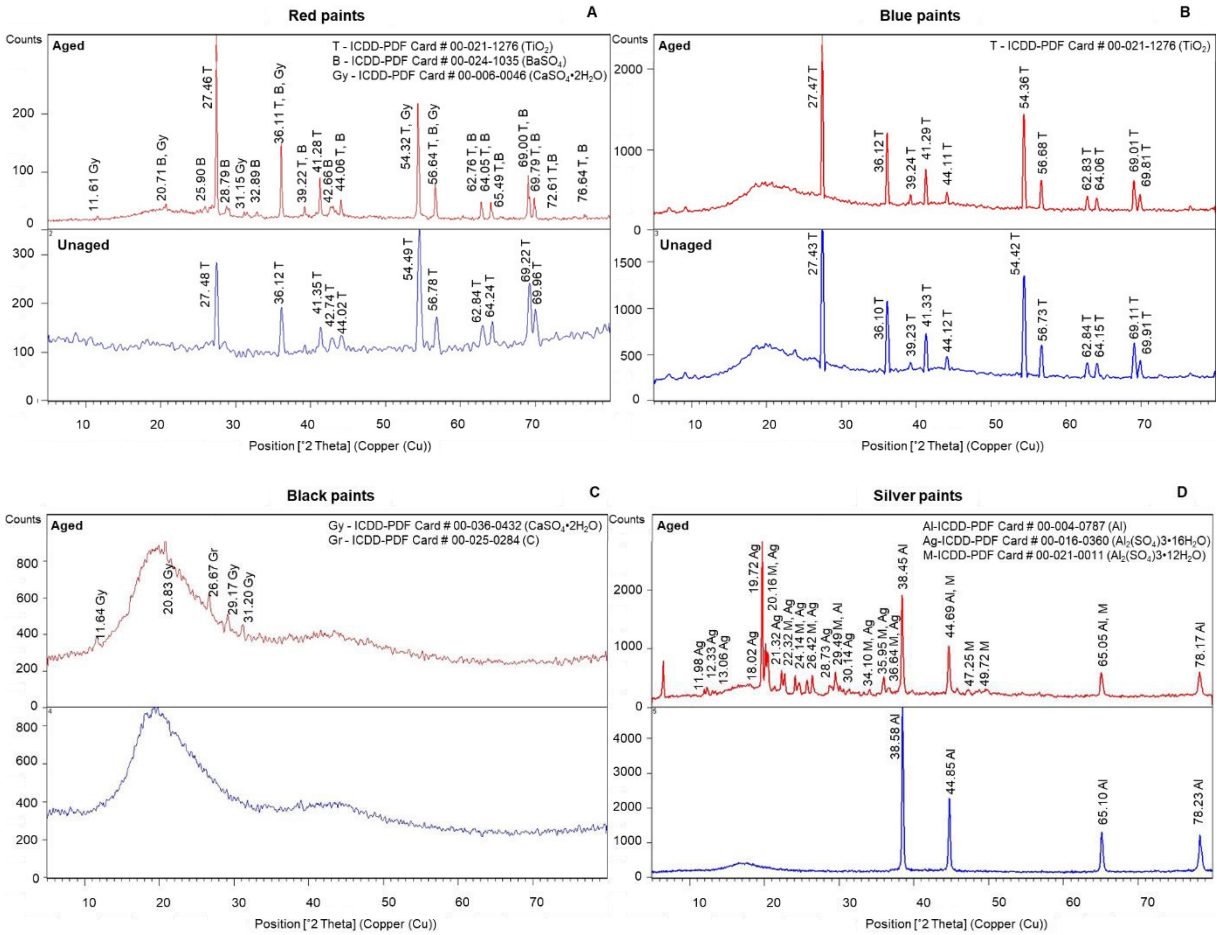
Fig.4.3 – Powder XRD pattern of aged (after SO_2 exposure) and unaged paints. A: Red paint. B: Blue paint. C: Black paint. D: Silver paint. Titania (T), gypsum (Gy), barite (B), graphite (Gr), aluminium (Al), alunogen (Ag) and metalunogen (M).
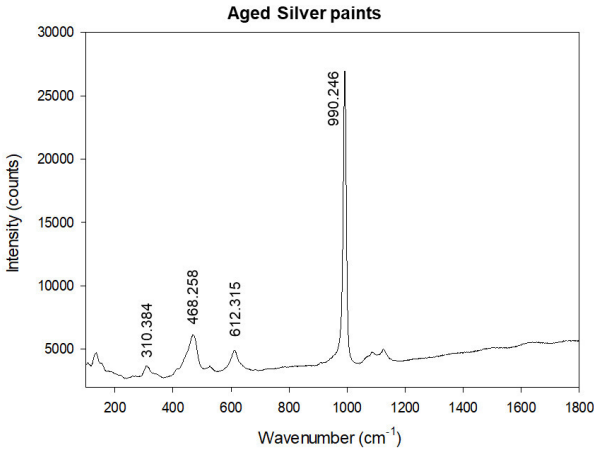
Fig.4.4 - Raman spectra for aged silver paint (after SO_2 exposure).

13

efflorescence crystals detected on silver paints (Fig.4.4). XRD allowed to detect graphite (C) in the aged black paint (Fig.4.3 C). Despite barite and graphite were only detected in the diffractograms of the aged samples, it was assumed that these compounds were also present in the unaged samples since barite is commonly used as an opacifier and graphite as a black pigment.

FTIR showed that the red, blue and black paints are composed of alkyd resins or varnishes (Fig.4.5 A, B and C) due to C-H and ester functional groups: C-H aromatic alkene around 3117 cm^{-1}, 3062 cm^{-1} and 740 cm^{-1}, C-H asymmetric and symmetric stretching vibrations of alkanes at 2925 cm^{-1} and 2854 cm^{-1} respectively, C=O vibrations around 1722 cm^{-1} and 1258 cm^{-1}, C=C aromatic ring at 1624-1481 cm^{-1}, C-H bend of CH$_2$ symmetric deformation
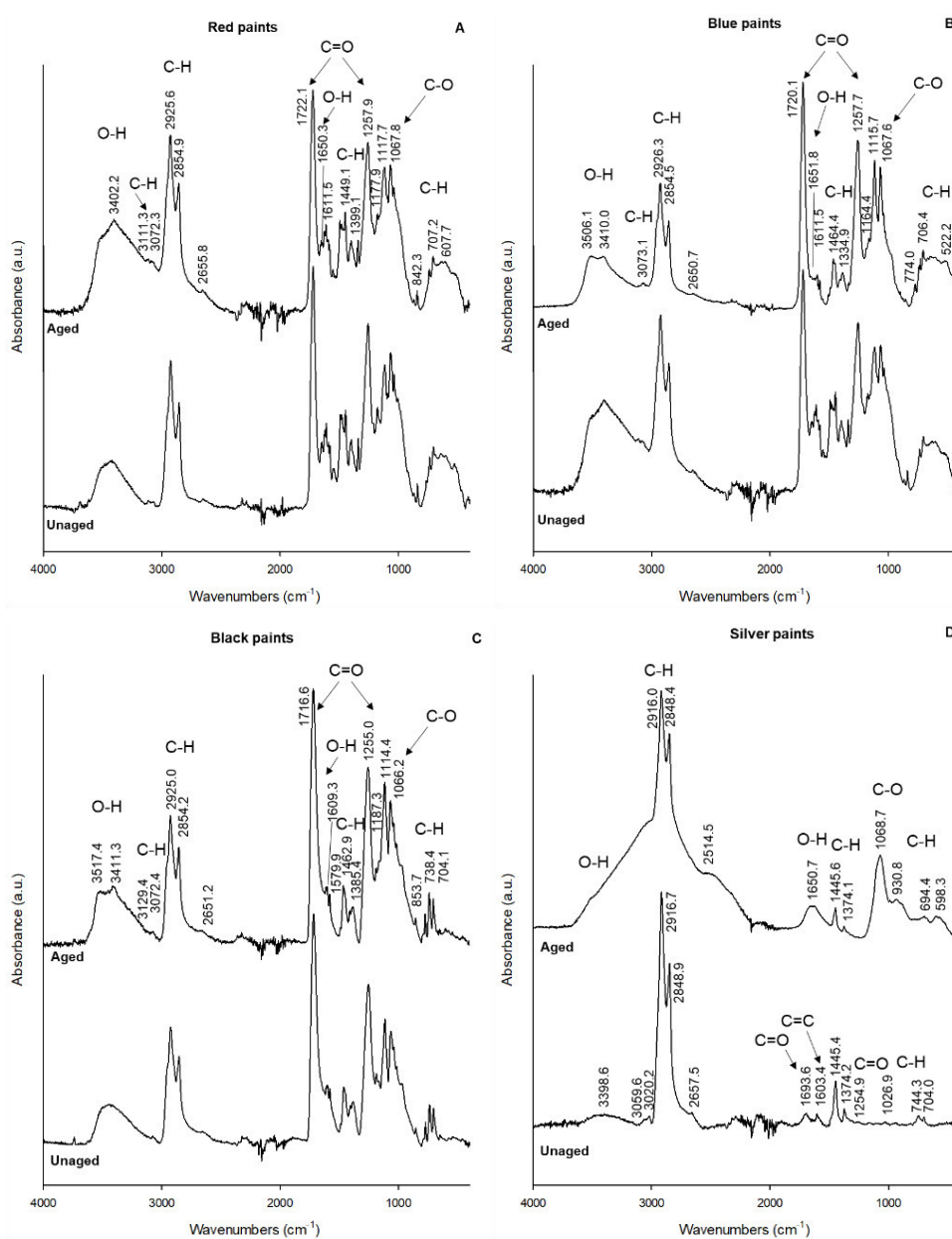
Fig.4.5 - FTIR spectra of aged (after SO$_2$ exposure) and unaged paints. A: Red paint. B: Blue paint. C: Black paint. D: Silver paint.

at 1448 cm^{-1}, CH$_3$ asymmetric deformation and vibrations around 870 cm^{-1} also attributable to C-H, C-O of ester at 1179 cm^{-1}, O-CH$_2$ phthalate vibration at 1117 cm^{-1} and C-O vibration at 1068 cm^{-1} [53,54]. Effects attributable to OH group were also detected: a broad band around 3482 cm^{-1} and around 1650 cm^{-1} [54]. The three paints were similar, except in the range of 740-529 cm^{-1}. For the silver paint (Fig.4.5 D) the most intense effects were those for C-H asymmetric stretch vibrations of alkanes. These C-H vibrations according to other authors [14] may be an indication of polyethylene polymers in this paint. These results are in agreement with previous characterizations of the same unaged paints [11,14]. On the one hand, it was possible to notice that the alkyd systems show greater resistance than the polyethylene ones towards moisturized SO$_2$ rich environments. On the other hand, FTIR spectrum of the aged silver paint allowed to identify some alteration signs, namely the disappearance of C=O, C=C groups and their substitution with a O-H group around 1650 cm^{-1} and the emergence of a C-O group around 1068 cm^{-1} [54].

By SEM observation of the paint surfaces (Fig.4.1) it was possible to observe the formation of sulphur compounds: (i) needles rich in S and Ca; and also Ti in paints rich in this element (Fig.4.1 B, C, H and I); (ii) agglomerates rich in S, Ca, Ti and Fe (Fig.4.1 E and F), plus Al in silver paints and Ba in red paints (Fig.4.1 B and C); and (iii) in silver paint also occurred the formation of ramifications rich in S and Fe (Fig.4.1 K and L), in which the Fe presence may be related to the oxidation process of the biotite. All the mentioned sulphur rich compounds presented a more limited development in the alkyd paints than in the polyethylene one as can be seen by the stereomicroscope images of the paints (Fig.4.1 A, D, G and J). The improvements in the alkyd resin properties may explain its higher resistance towards sulphur rich environments in comparison to polyethylene ones. In what concerns the binders field, there are indicators that alkyd resins had been subject to many blending, modification and formulation transformations [55].

The cross-cut test allowed to qualitatively assess the adhesion of the paint according with the amount of detached material (Figure 4.6). The tested paints presented different adhesion degrees, blue and black paints registered the maximum adhesion (0). Silver paint
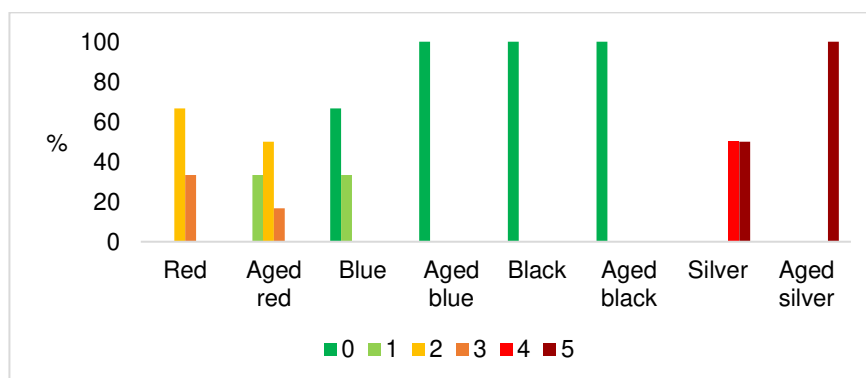
Figure 4.6 - Cross-cut adhesion test according to UNE-EN-ISO-2409 standard of the unaged and aged (after SO$_2$) paints.

presented the lowest adhesion (5), which is in agreement with the macroscopic deterioration of the paint and crystallizations formation. Red paint is the middle ground between these values. The paints did not presented significant adhesion alterations towards SO_2 exposure.

4.2. Cleaning performance

The application time of each cleaning procedure was controlled in different manners: 1) in the chemically cleaned samples, under naked eye observations the experimented worker decided when the cleaning would not achieved an improvement with another application with a maximum of 5 applications and it was detected that the aged samples need around 1-2 passages more to be cleaned than the unaged samples (Appendix 7.8); 2) in the mechanically cleaned samples, the application of the methods was controlled through the timing being needed the double time for the aged samples (Appendix 7.8); and 3) the laser cleaning was also controlled through naked eye observations and were applied the same number of passes since at first sight the results were similar.

Stereomicroscopy allowed to perform the first evaluation of the cleaning in terms of graffiti extraction. Regarding the chemically cleaned aged samples (Fig.4.7 C and E), more residues were found on the surfaces comparatively to the cleanings of unaged ones. Two different paint residue patterns related to each chemical cleaner method were found for both unaged and aged samples. While *AGS* acted in the graffiti through dissolution by saponification, leaving behind sporadic lines of paint, *GR3* crackled the paint film, leaving as result not only sporadic lines of paint as also some paint "islands" in areas probably with higher adherence of the paint layer to the stone. In fact, the triglycerides of the alkyd paints (red, blue and black) when interact with a strong base (alkaline solution such as *AGS*) trigger a chemical reaction known as saponification, the cleaner composed of KOH acts as a source of OH⁻, a highly nucleophilic anion that attacks polar bonds, catalysing the cleavage of the ester bonds, releasing fatty acids salts and glycerol [56]. However, *GR3* appears to act by weakening the adhesion between the paint and the substrate. The mechanically cleaned samples (Fig.4.7 G, I, L and N) showed less residues than the chemically cleaned samples, but an increase in morphological alteration was detected, which may be associated with morphological alterations, later confirmed by the roughness tests. The aged laser cleaned samples (Fig.4.7 P) presented a surface with more colour differences and residues in relation to the unaged samples, this was particularly evident in the case of blue and black paint with a more demarked veil of graffiti colour associated with quartz mineral and in the case of silver paint with a glossy silver veil which after ageing also presented crystallizations. Macroscopically, the best chemical and mechanical cleaning performances were achieved with *AGS* and *Hydro* respectively (Fig.4.7).

16

SEM allowed to perform a more detailed analysis of the cleaned surfaces. Graffiti residues on the surface were identified due to the presence of deposits or particles rich in C, Na, Mg, Al, Cl, Ca, Ti, due to their presence in the composition of the paints. Therefore, they were used as markers to identify paint residues by EDS. SEM analysis (Fig.4.7 A and Appendix 7.9) of aged unpainted substrates confirmed the presence of crystals rich in sulphur. Once quartz and alkali feldspars (Na and K) are amongst the most resistant silicates to acid media they showed little decay under SO_2 conditions [44]. This can explain the limited development of crystals in Rosa Porriño granite (Fig.4.7 A). The development of sulphates around the particulate matter in a SO_2 environment and their absence on environments with only SO_2 (without particulate matter) were reported by Simão *et al.*[44]. Well-developed gypsum crystals associated to particulate matter emitted from motor vehicles (diesel and leaded gasoline) in a SO_2 environment were found in Monção granite (calc-alkaline, one mica, medium coarse grained, pink colour) [44], mineralogical and texturally similar to Rosa Porriño. The particulate matter may play a critical role in the sulphation. These appear to contribute to the catalytic oxidation of SO_2 to H_2SO_4 in the presence of humidity since their nanoparticle size provides a surface area that potentiates the sulphation [44].

As far as the cleaning is concerned, both aged and unaged chemically cleaned samples (Fig.4.7 D and F) presented only punctual residues of graffiti paint with *AGS* (Fig.4.7 D) and besides the punctual residues some bigger paint plaques with *GR3* (Fig.4.7 F). Pozo-Antonio *et al.* tested QuitaGraffi 200®–QuitaSombras 60® (QG+QS) rich in potassium hydroxide and Wendrox® and Eligraf® based on dichloro-methane, organic acids, solvents and anionic surfactants on Silvestre and Rosa Porriño granites [13]. The products based on potassium hydroxide were, the most effective in removing the red, blue, black and silver Montana Colours®, however chemical contamination occurred with both Wendrox® and QG+QS [13]. Conversely, in the current study were not found any mineralogical alterations or residues of the cleaners. However, the evaluation of cleaning performance through SEM-EDS in granitic surfaces cleaned with potassium hydroxide-based products must be taken with caution because K is present in the granite forming minerals and also in the cleaners. The aged samples showed surfaces characterized by the presence of more paint residues and sulphur. So, despite macroscopically the majority of the paints appeared unaltered after ageing, the sulphur dioxide interacted with them.

SEM allowed to detect that the surfaces of the samples cleaned with the mechanical methods had greater influence on the surface morphology (Fig.4.7 H, J, M, O) comparatively to chemical cleanings. Moreover, the presence of paint residues seems to be related with the
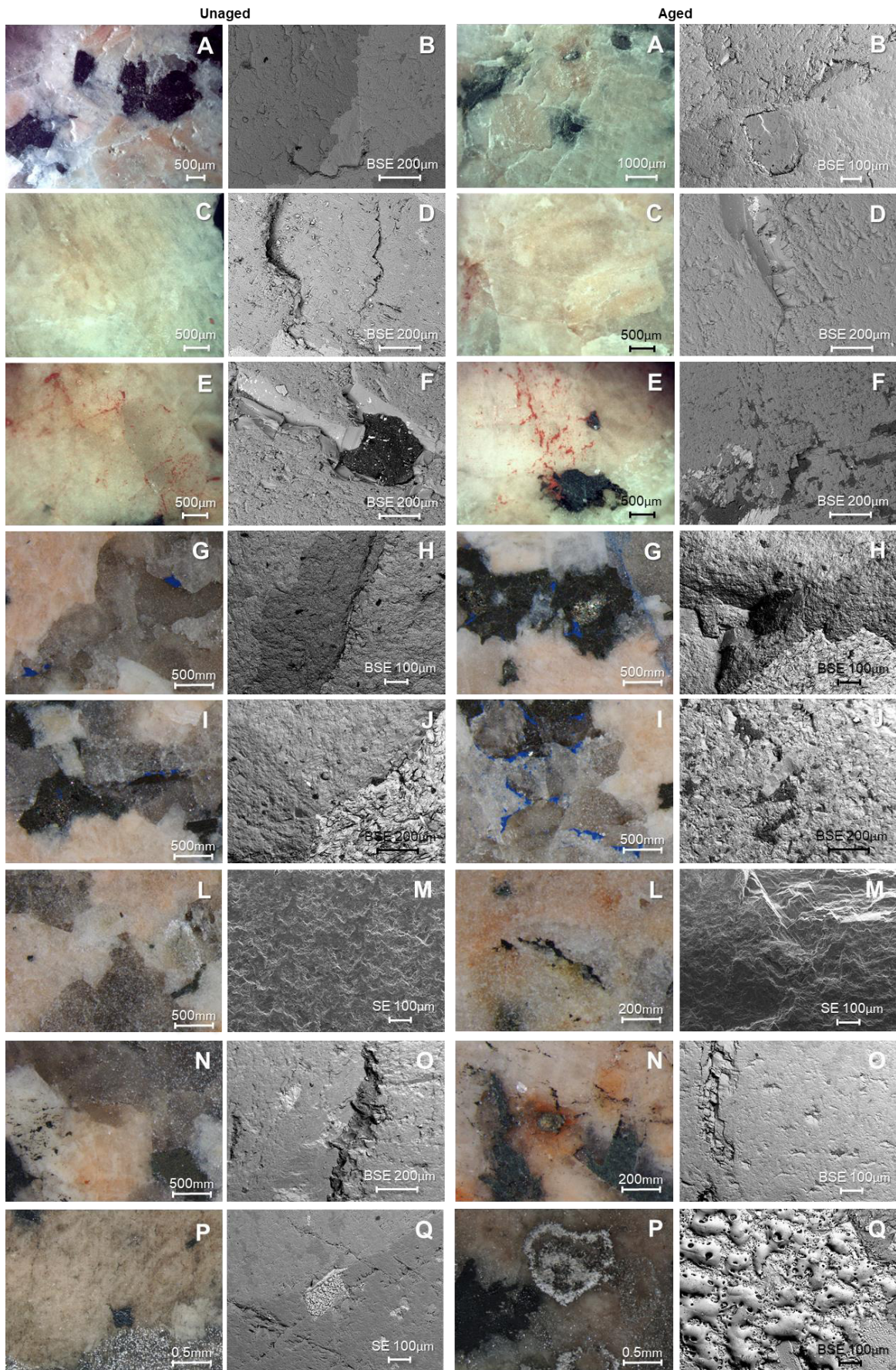
Unaged   **Aged**

Fig.4.7 – Stereomicroscopy- and SEM-micrographs of the unaged and aged (after SO_2 exposure) cleaned surfaces. A-B: Reference granite. C-D: Red paint with *AGS*. E-F: Red paint with *GR3*. G-H: Blue paint with *Hydro Si*. I-J: Blue paint with *Hydro Si Al*. L-M: Black paint with *IBIX Si*. N-O: Black paint with *IBIX Ca*. P-Q: Silver paint with *Nd:YVO$_4$*.

18

morphological alterations of the surface. The lesser the residues, the higher the morphological alterations, since more effort was put in order to remove them. The satisfactory results were obtained through the best compromise between extraction and safeguard of the polymineralic granitic substrate. *Hydro* both with *Si* and *Si Al* (Fig.4.7 H and J) appeared to be the one with the best results, as referred by previous authors [13]. *IBIX Si* (Fig.4.7 M) induced the higher morphological alterations and lesser paint residues, and in contrast, *IBIX Ca* (Fig.4.7 O) was the one with more paint residues. For the mechanical cleaning of the aged samples, longer cleanings could be translated in more evident morphological alterations than those registered on the mechanically cleaned surfaces with unaged paints.

On the surfaces cleaned with laser, the graffiti residues were not so evident as on the surfaces cleaned with chemical and mechanical procedures (Fig.4.7 Q) since the ablation removal mechanism allowed a more homogeneous cleaning [33]. As reported by other authors [13,14], despite satisfactory results were found in the cleaning of red, blue and black paints, the cleaning of silver paint left surfaces with residues rich in Al. regarding the induced damages to the granite forming minerals, despite the low fluences applied [40] alterations of biotite were observed, namely melting of the biotite grains (Fig.4.7 Q) as was reported in [13,14]. Recently, Ramil *et al.* reported the biotite melting (similar to drops) for even the lowest fluence tested of 0.06 J.cm^{-1} [40]. Nevertheless, it must also be noticed that no other mineral alterations such as spallation or melting of feldspar planes and quartz fracture [11,14] were observed. The effect of ageing through SO_2 exposure on laser cleaning was not so evident as on the other cleaning procedures. In fact, the cleaning conditions applied were the same, since at first sight the results were similar, however through the analytic techniques it was seen that the cleaning was not exactly the same. In fact, for the cleaning of aged silver graffiti was observed that the white crystallizations rich in Al and S formed after the ageing process, still remained on the surface after the cleaning process. So, the SO_2 exposure hindered the laser cleaning process.

The colour changes of the chemically cleaned samples comparatively to the reference granite surfaces (without graffiti) mainly affected L* (decreases- surfaces became darker) (Fig.4.8 A and B) and a* (decreases-surfaces became less reddish) (Appendix 7.10). On the surfaces cleaned of blue, black and silver graffiti, a* decreases can be related with the improvement of the cleaning, while in the cleaning of red graffiti, a* increases can be related to paint residues. However, b* coordinate remained similar to the reference. The chroma C^*_{ab} decreased in all cases, again with exception of red paint which tone appeared to intensify due to the colour of the residues. In the Fig.4.8, can be noticed that *AGS* (Fig.4.8 A) induced less colour alterations than *GR3* (Fig.4.8 B). The global colour changes ΔE^*_{Lab} (Table 4.2) are generally above 5 for all colours, which means that the observer notices two different colours [48]. *AGS* had better cleaning results, presenting a lower computed residue percentage (R, %) (Table 4.1), except for the silver paint whose difference can be related to its chemical nature.
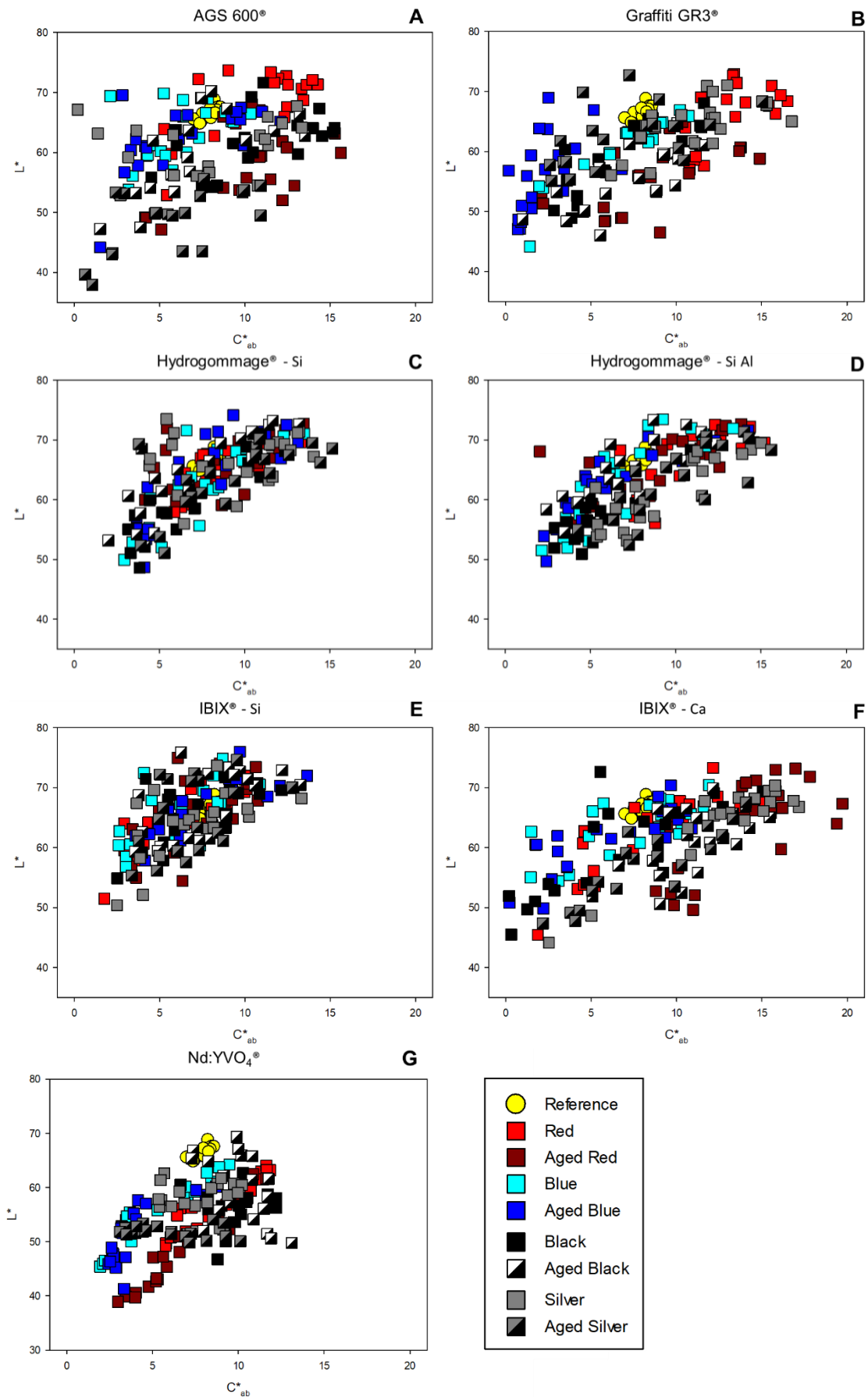
Fig.4.8 - L*–C*$_{ab}$ data obtained for the granite reference and aerosol-painted surfaces after each cleaning procedure: A: AGS; B: GR3; C: Hydro Si; D: Hydro Si Al; E: IBIX Si and F: IBIX Ca; G: Nd:YVO$_4$.

It must be added that *GR3* applied solely on the stone showed higher colour modifications than *AGS* (Appendix 7.10).

The mechanically cleaned samples (Fig.4.8 C-F), in general maintained the L*, a*, b* and C*$_{ab}$ around the reference values, with exception of the silver sample cleaned with *Hydro Si Al* (Fig.4.8 D), which increased in all coordinates and *IBIX* cleaned samples (Fig.4.8 E and F) which decreased in all coordinates. The mechanical methods that induced less colour alterations were *Hydro Si* (Fig.4.8 C), confirming [13], and *IBIX Si* (Fig.4.8 D). In general terms, their ΔE*$_{Lab}$ can be noticed by an unexperienced observer [48] but are lower than those registered on the chemically cleaned surfaces (Table 4.1), except for the surfaces cleaned with *IBIX Ca* (Fig.4.8 F) showing the worst results. In fact, the mechanical methods were the ones that achieved less computed residue percentage (R, %). However, it must be noticed that these methods induced macroscopic morphological alterations due to their abrasive mechanism, especially *IBIX*. ΔE*$_{Lab}$ of the surfaces with unaged graffiti and mechanically cleaned are between 0.40 and 8.90, which are lower than those obtained by Carvalhão & Dionísio (above 10) with soft-abrasive blasting media in two carbonate stones [21].

The laser cleaning (Fig.4.8 G) induced an increase of L* and decreases of a* and b* for surfaces cleaned of red and blue graffiti paints and surfaces cleaned of black and silver paints exhibited increases of a* and b*; moreover, the surfaces cleaned of silver paint showed L* decreases. C*$_{ab}$ did not experiment a clear trend. The ΔE*$_{Lab}$ of laser cleaned surfaces were the highest in comparison with the other cleaning methods (Table 4.1) and therefore, the observers would notice the unsatisfactory cleaning by laser due to the residues presence [48]. The computed residue percentage (R, %) showed the same trend that the ΔE*$_{Lab}$, especially for silver graffiti achieving an average residue percentage of 34.52% and of 66.07% for unaged paint and aged paint respectively. This unsatisfactory cleaning of silver paint in contrast with the other paints was reported in [11,13,14].

The results obtained for all the referred cleaning methods allowed to infer that the cleaning of aged samples led to higher ΔE*$_{Lab}$ comparatively to unaged ones, with values above 3.5 in the cleanings of all colours. The most successful cleaning methods for aged samples were the same as for the unaged samples, being more difficult to remove than the unaged graffiti and with a higher residue percentage associated. It is evident that SO$_2$ hindered the cleaning performance for all the cleaning methods

In a previous work the suitability of hyperspectral imageing technique to detect variations in the reflectance of granite samples after laser cleaning was verified [40]. In the current research, the higher the α_{LSOSP}, the more similar the reflectance of the cleaned surface to the reference granitic surface (without graffiti). Generally, it was detected that the cleaned surfaces of unaged graffiti showed a higher or equal α_{LSOSP}, than their aged graffiti counterparts (Table 4.1). However, some exceptions were detected where the unaged cleaned samples presented

lower α_{LSOSP} than the aged ones. This occurred in red paints cleaned with *Hydro Si*; in blue paints cleaned with *GR3*, *Hydro Si*, *IBIX Si*, *IBIX Ca*; for black paints cleaned with *AGS*, *Hydro Si*, *IBIX Ca* and for silver paint cleaned with *Hydro Si*. From the obtained results can be concluded that the mechanical methods, based in micro abrasive removal mechanisms, among all the tested methods, are the less dependent on the graffiti ageing. It was also detected that the lowest α_{LSOSP} were obtained on the surfaces cleaned by laser which is translated into a surface with more paint residues.

Table 4.1 – Colorimetric average data: the degree of colour difference ΔE*Lab (-), residue percentage: R (%) and abundance coefficient: α*Gmi* (-) for the chemical, mechanical and laser cleaning procedures. The prefix A marks the samples that were subjected to ageing before the respective cleaning procedure.

Cleaning methods	Red paints			Blue paints			Black paints			Silver paints		
	ΔE*Lab (-)	R (%)	α_{LSOSP} (-)	ΔE*Lab (-)	R (%)	α_{Gmi} (-)	ΔE*Lab (-)	R (%)	α_{LSOSP} (-)	ΔE*Lab (-)	R (%)	α_{LSOSP} (-)
AGS	3.60	7.70	1.10	4.10	8.50	0.90	5.50	13.00	0.80	6.30	25.90	0.80
A-AGS	9.60	20.70	0.80	4.60	9.70	0.90	7.10	17.00	1.00	18.50	75.60	0.80
GR3	5.30	11.50	0.90	5.10	10.60	0.70	7.90	18.90	1.10	3.80	15.40	1.10
A-GR3	10.90	23.60	0.80	11.90	24.90	1.00	10.50	25.10	0.70	4.60	18.90	0.80
Hydro Si	1.90	4.10	0.80	0.80	1.70	0.80	2.10	5.10	0.80	0.60	2.60	0.80
A-Hydro Si	4.10	8.80	1.00	2.20	4.60	0.90	3.00	7.20	1.00	2.70	11.20	0.90
Hydro Si Al	2.50	5.40	1.00	2.30	4.70	0.80	3.80	9.00	0.80	5.80	23.90	1.10
A-Hydro Si Al	3.30	7.00	1.00	2.10	4.40	0.80	4.50	10.70	0.70	5.90	24.30	1.00
IBIX Si	0.80	1.70	1.00	0.40	0.80	0.90	1.90	4.40	0.90	1.80	7.20	0.80
A-IBIX Si	2.00	4.30	0.90	2.30	4.80	1.00	2.70	6.50	0.90	2.60	10.50	0.70
IBIX Ca	3.30	7.20	0.90	1.30	2.70	0.80	2.30	5.50	0.90	5.90	24.30	1.60
A-IBIX Ca	8.90	19.20	0.90	3.20	6.70	0.90	6.30	15.00	1.00	7.60	31.20	0.90
Nd:YVO₄	13.10	28.30	0.70	12.20	25.40	0.70	10.99	26.18	0.80	8.43	34.52	0.60
A-Nd:YVO₄	19.60	42.20	0.60	16.40	34.20	0.60	11.31	26.94	0.70	16.13	66.07	0.10

The analysis of surface roughness values (Appendix 7.11) showed that after painting the stone samples generally occurred a Ra decrease (Fig.4.9). It is assumed that the paint created a film that filled the valleys of the stone, smoothing the surface. Except for silver paint which slightly increased this parameter (2.635 µm), indicating that this paint forms a heterogeneous coating. For the aged samples, a significant increase of silver paint Ra was registered (10.646 µm), being this probably related with the development of sulphur aggregates in the surface of the paint. For the chemically and laser cleaned samples, there were no statistical evidence of existing differences between Ra of the reference stone and after the cleaning (pvalues>0.05). Similar results were reported by Carvalhão & Dionísio in the cleaning of Branco marble and Lioz limestone with a commercial cleaner based on potassium hydroxide [21] and by Pozo-Antonio *et al.* with Nd:YVO₄® at 355 nm laser cleaning of Rosa Porriño and Silveste granites [13]. This was particularly curious in the case of the samples cleaned with *AGS* due to

its high pH. The reference granite cleaned with the laser after SO_2 ageing showed roughness alterations statistically higher than those registered on the stone reference without SO_2 exposure which can be related to the decay promoted by SO_2 attack. In contrast, Ra of the majority of the mechanically cleaned surfaces, except those cleaned with *IBIX Ca* showed pvalues ≤ 0.05 and thus, there were significant differences between the Ra of the reference stone and the values registered after cleaning, with a confidence interval of 95%. Therefore, mechanical procedures were the methods that induced greater surface roughness changes.

In addition and in order to evaluate the extent of the topographical variations that could be accepted as a result of a cleaning treatment, a similar methodology to Gaspar *et al.* was implemented [52]. As was previously described, based on the Ra values, a damage threshold of 2.853 µm was computed. As can be seen in Fig.4.9 the roughness damage attributed to the cleaning performance (*2) were often coincident with the detected significant differences between the reference and after cleaning, to reject the null hypothesis with a confidence interval of 95% (*1). For the mechanical methods three deductions were made: (i) *IBIX Ca* induced some roughness alterations associated with damage, despite these were not evidenced by the statistical calculations; (ii) After *IBIX Ca*, *Hydro Si* exerted lower impact on surface roughness; conversely to other authors working with Silvestre and Rosa Porriño granites [13] Ra increased around 3 orders of magnitude less; (iii) *IBIX Si* showed the highest mechanical damage since Ra increased ≈4 µm on the unaged surfaces and ≈5 µm on the aged surfaces. It was not possible to find any relation between surface roughness and cleaning performance after SO_2 exposure, except for the laser cleaning, once the same cleaning conditions were applied for
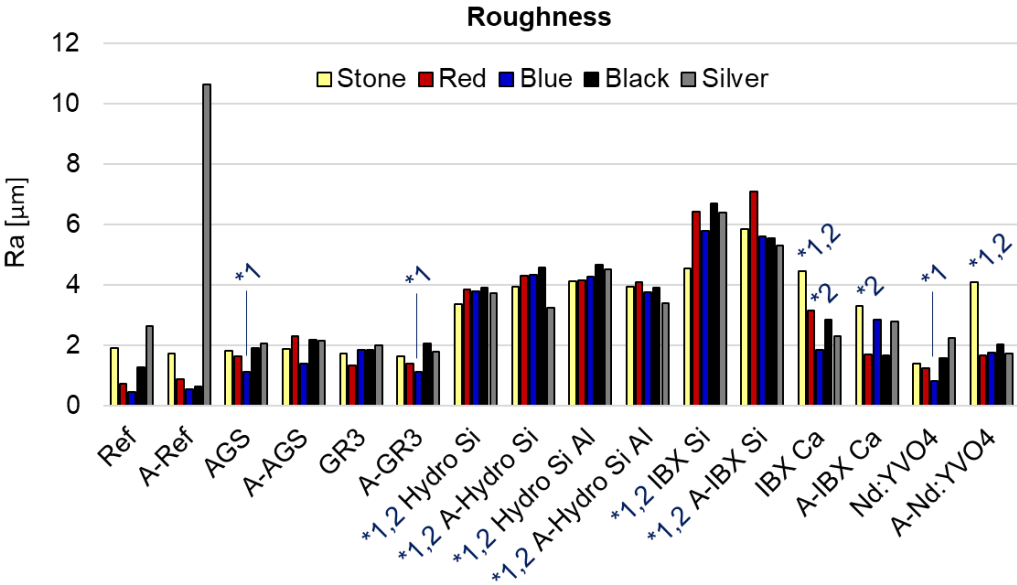
Fig.4.9 – Ra (average roughness) for aged (after SO_2 exposure) and unaged samples before and after the cleaning procedures. The prefix A marks the samples that were subjected to ageing before the respective cleaning procedure. *1: Significant differences between the reference and after cleaning. *2 Roughness damage attributed to the cleaning performance.

aged and unaged samples and more residues were found in the laser cleaning of aged samples.

Considering the confocal microscopy, a clear difference between the surfaces morphology can be noticed by the 3D images (Fig.4.10), being the highest morphological alterations detected in the surfaces cleaned with *IBIX Si* (Fig.4.10 D). A more homogeneous surface was obtained with *AGS* (Fig.4.10 B) and *Nd:YVO₄* (Fig.4.10 E)*, despite some localized mineral alterations were detected on the surface cleaned with the later, *Hydro Si* (Fig.4.10 C) represents the middle ground between these extremes. So, these results are in agreement with the ones obtained with Ra roughness.
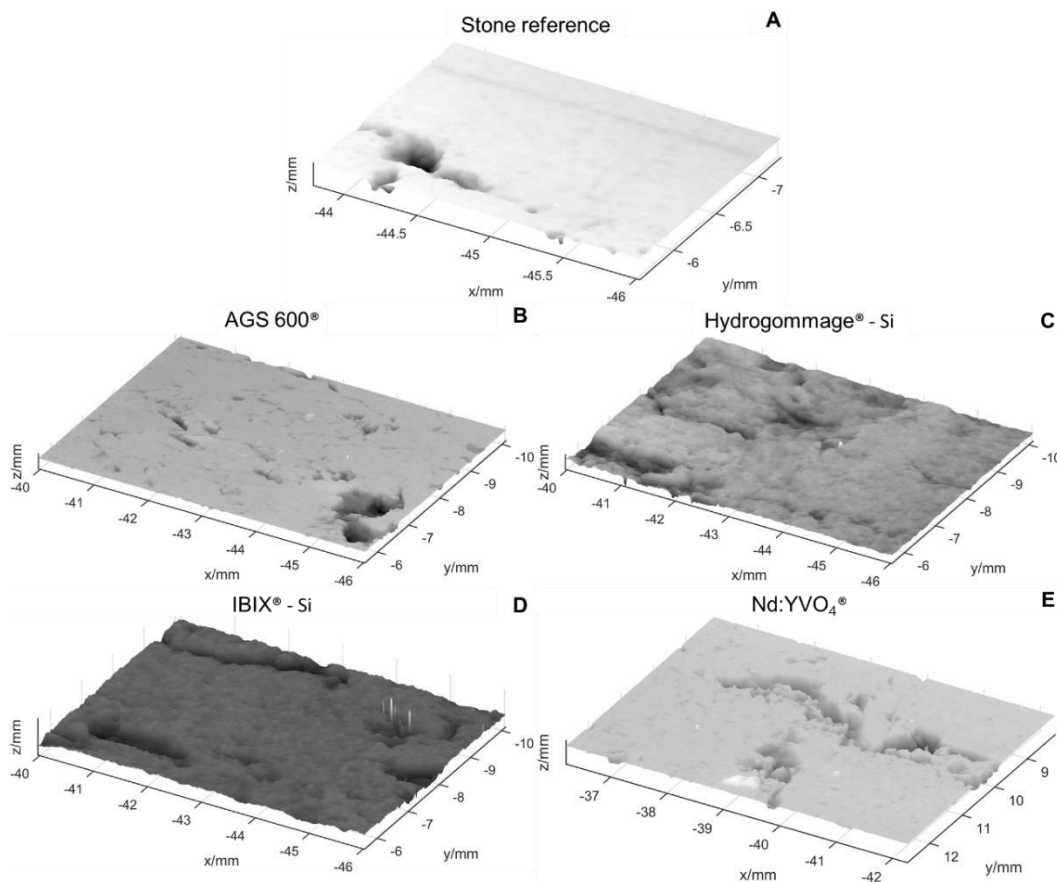
Fig.4.10 – 3D images obtained though confocal microscopy data of some different surfaces: reference stone (A) and surfaces cleaned of aged black graffiti with *AGS* (B); *Hydro Si* (C); *IBIX Si* (D) and Nd:YVO₄ (E).

In what concerns the static contact angle (Fig.4.11 and Appendix 7.12), in first place must be mentioned that since granite is a polymineral stone with grains of different compositions and characteristics, the static contact angles necessarily reflect this heterogeneity by means of variable results. Besides this, it must also be taken in consideration the Rosa Porriño fissural system, characterized by the three different fissures (transgranular, intergranular and intragranular) [57]. So, it was decided to present these measurements in a graph containing the minimum and maximum intervals and average values (Fig.4.11).

First of all, must be noticed an increase of the hydrophobic behaviour after the application of all the paints without achieving surface hydrophobization, as reported by other authors with

alkyd paints applied in Branco marble and Lioz limestone [10,21,22]. According to Dionísio & Ribeiro and Ribeiro *et al.* the aerosol paints filled the stone surface irregularities, creating a smooth and uniform overcoat, acting as an impermeabilizing agent and keeping the stone from interacting with its surrounding environment [10,22].

These static contact angles had a tendency to decrease after the cleaning procedures, contrary to the results obtained by Carvalhão & Dionísio [21]. In fact, these authors considered that those higher values were related with traces of unremoved paint absorbed in some of the stone pores [21]. After the cleaning procedures *Hydro Si* was, on the one hand, the method that achieved the closest results to the stone reference. On the other hand, *IBIX Si* was the method that achieved surfaces with contact angle more distant to the reference; this method promoted a higher increase in the roughness values. Therefore, it may be inferred a relationship between the static contact angle and the roughness, since a rougher surface will present more cracks and fractures that will facilitate the water penetration. The aged stone surface became more hydrophobe, (in some cases exceeding the 90˚), a slight increase of the static contact angles also occurred with Branco marble and a higher one with Lioz limestone when submitted to SO_2 [10,22].

After the ageing, in the present study, the painted samples decreased their
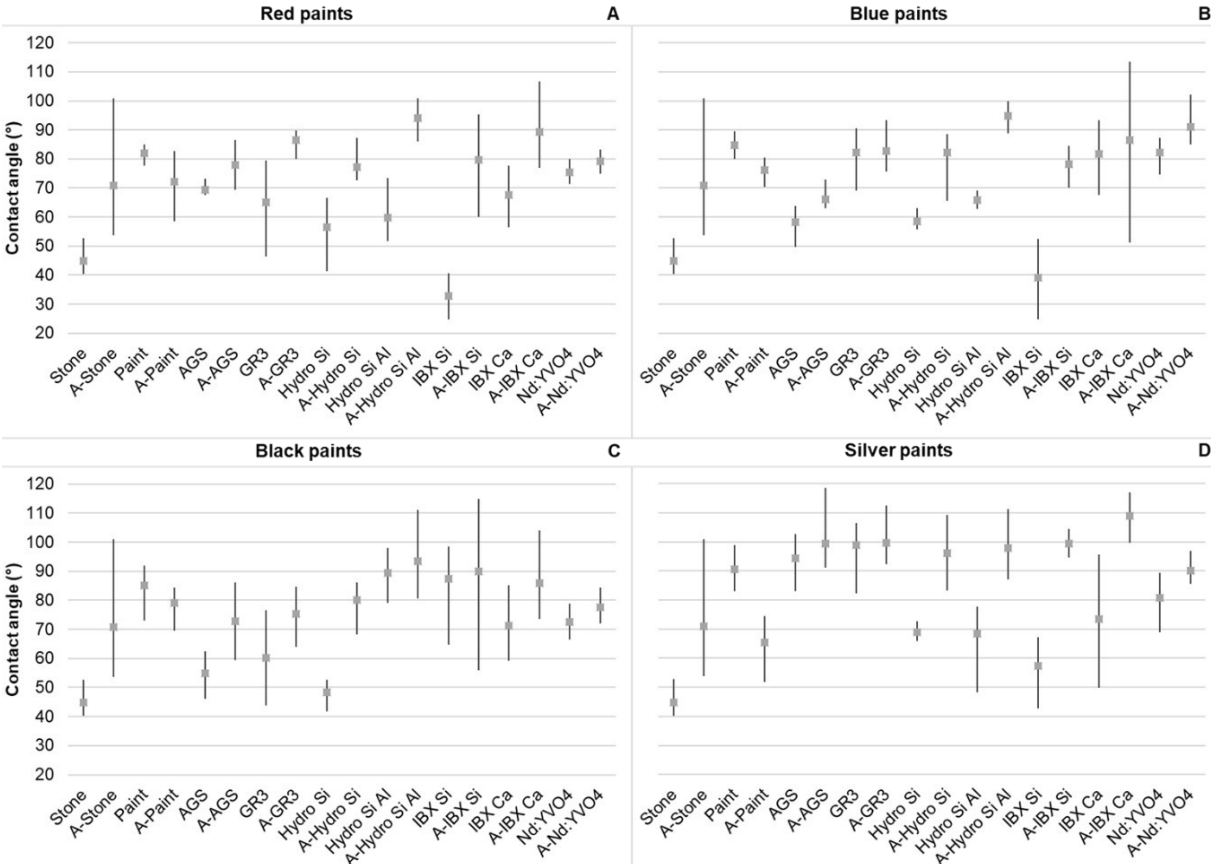
Fig.4.11 - Static contact angle represented in intervals of minimum, maximum and average for the unaged and aged (exposed to SO_2) cleaned samples. A: Red paint. B: Blue paint. C: Black paint. D: Silver paint. The prefix A marks the samples that were subjected to ageing before the respective cleaning procedure.

hydrophobicity, which was the opposite of what occurred with the referred Branco marble and Lioz limestone coated with alkyd paints [10,22], the authors reported increases in the static contact angles and water vapour permeability after the artificial ageing.

After the cleaning procedures of the aged samples, the surfaces became more water repellent. This allows to think that the SO_2 had the ability to interact with the stone (became more water repellent), interact with the coating (decreased hydrophobicity since degraded the coating and allowed the entrance of water) and promoted interactions in the interface stone-coating since a more water repellent pattern was observed after the cleaning processes. Must also be taken in consideration that the contact angles increase after cleaning may be related with traces of unremoved paint covering the granite fissures. After cleaning a SO_2 aged surface, the static contact angle results are closer to the aged granite and not to the reference granite. This allows to infer (in agreement with the observation of water droplets on the samples surface) that SO_2 may play a critical role in surface hydrophobization. Silver aerosol paint differentiates from the other aerosol paints by its higher static contact angles, even after the cleaning procedures.

5. Final remarks

Four aged and unaged graffiti aerosol paints (red, blue, black and silver) were evaluated in order to characterize their ageing process. These aerosol paints were tried to remove from a granite substrate with chemical, mechanical and laser technologies in order to optimize the graffiti removal procedures on samples subjected to SO_2 environment (one of the more common urban contaminants).

Red, blue and black paints had alkyd resins in their formulation whereas silver paint had polyethylene ones. Alkyd paints presented a greater resistance than polyethylene ones towards moisturized SO_2 rich environments. Despite the formation of sulphur rich compounds in all paints, these had a more limited development in the alkyd paints than in the polyethylene one (silver). The silver paint was the one that presented more alteration signs, namely the disappearance of C=O, C=C groups, their substitution with an O-H group, emergence of a C-O group. These chemical alterations were followed by the formation of an unexpected mineral phase: alunogen in the form of crystals. The cleaning performance of chemical and laser methods was dependent on the binder composition (alkyd or polyethylene resins) and the pigments composition, namely the Al presence in silver paint.

Chemical methods induced higher global colour changes and lesser roughness alterations. *AGS* based on KOH, showed a satisfactory cleaning since it acted through the alkyd resins by saponification, effectively dissolving the paints, except for the silver paint which achieved better results with *GR3*. Comparably to *GR3* also induced less colour modifications.

Mechanical methods achieved higher extraction levels of graffiti, leading lesser paint residues on the samples surfaces than the chemical ones, but with a macroscopic morphological alterations increase, revealing an increase in roughness, the higher from all the tested methods. The global colour changes and the residue percentages were the lowest among all the tested methods. *IBIX Si* induced high morphological alterations in such a way that a brighter abraded surface was noticed. *IBIX Ca* despite induced lower morphological alterations it left high residue percentage. *Hydro Si* induced the lowest colour alterations and in terms of morphologic alterations this method is placed between the chemical and the laser (the lowest morphological changes induced) and *IBIX Si* (the highest morphological changes induced). Among the other cleaning methods, *Hydro Si* was the one which surface hidrophocity resembled more to the reference stone.

The laser method Nd:YVO$_4$ left coloured veils of blue, black and a more evident one of silver paint. Higher global colour changes, residue percentage and reflectance modification were verified, being highest changes for all the tested methods, especially in the case of silver paint. However, few morphological alterations were registered.

In general terms SO$_2$ clearly influences the cleaning performance for all the cleaning methods. The aged cleaned surfaces were more difficult to clean (needed more passages and required more time), presented higher global colour changes and showed a higher residue percentage. A more water repellent surface was also verified after ageing; the cleaned surfaces after SO$_2$ exposure showed static contact angles closer to the aged granite than to the reference granite which profs the influence of SO$_2$ on the graffiti and the stone.

Further studies focused on the cleaning performance of aged graffiti paintings with particulate matter emitted from motor vehicles should be developed since it may play a critical role in the sulphation process. This research should also be extended to more stone substrates, such as carbonate ones: limestone and marble very employed in Cultural Heritage and less studied silicate ones like sandstones.

6. References

[1]   English Heritage, Graffiti on historic buildings and monuments. Methods of removal and prevention., English Herit. (1999) 1–12. http://www.english-heritage.org.uk/.

[2]   GRAFFITAGE, GRAFFITAGE: Development of a new anti-graffiti system, based on traditional concepts, preventing damage of architectural heritage materials. SSP (Policy Oriented Research) of the Sixth European Programme of the European Commission. FP6-2003-SSP3-513718, 2008.

[3]   GRAFFOLUTION, GRAFFOLUTION: Awareness and Prevention Solutions against Graffiti Vandalism in Public Areas and Transport. SSP (Policy Oriented Research) of the Seventh European Programme of the European Commission. FP7-SEC-2013-1, 2016.

[4]   J.S. Pozo-Antonio, T. Rivas, A.J. López, M.P. Fiorucci, A. Ramil, Effectiveness of granite cleaning procedures in cultural heritage: A review, Sci. Total Environ. 571 (2016) 1017–1028. doi:10.1016/j.scitotenv.2016.07.090.

[5]   P. Sanmartín, F. Cappitelli, R. Mitchell, Current methods of graffiti removal: A review, Constr. Build. Mater. 71 (2014) 363–374. doi:10.1016/j.conbuildmat.2014.08.093.

[6]   V. Gomes, A. Dionísio, J.S. Pozo-Antonio, Conservation strategies against graffiti vandalism on Cultural Heritage stones: protective coatings and cleaning methods, Prog. Org. Coatings. 113 (2017) 90–109.

[7]   D. Urquhart, The treatment of graffiti on historic surfaces. Advice on graffiti removal procedures, anti-graffiti coatings and alternative strategies. Historic Scotland technical advice note no.18., Historic Scotland, Edinburgh, 1999.

[8]   ICOMOS, ICOMOS-ISCS : Illustrated glossary on stone deterioration patterns., Champigny/Marne, France, 2008.

[9]   P. Sanmartín, R. Mitchell, F. Cappitelli, Evaluation of Cleaning Methods for Graffiti Removal, Second, London: Imperial College Press (ICP)., 2015.

[10]   T. Ribeiro, A. Dionísio, L. Aires-Barros, Aerosol-paint graffiti: the effects on calcareous stone, Restor. Build. Monum. 15 (2009) 51–66.

[11]   M.P. Fiorucci, J. Lamas, A.J. López, T. Rivas, A. Ramil, Laser cleaning of graffiti in Rosa Porriño granite, in: M.F.M. Costa (Ed.), Proc. SPIE - Int. Soc. Opt. Eng., SPIE, 2011: p. 80014A–80014A–8. doi:10.1117/12.892158.

[12]   M.P. Fiorucci, A.J. López, A. Ramil, S. Pozo, T. Rivas, Optimization of graffiti removal on natural stone by means of high repetition rate UV laser, Appl. Surf. Sci. 278 (2013) 268–272. doi:10.1016/j.apsusc.2012.10.092.

[13]   J.S. Pozo-Antonio, T. Rivas, M.P. Fiorucci, A.J. López, A. Ramil, Effectiveness and harmfulness evaluation of graffiti cleaning by mechanical, chemical and laser procedures on granite, Microchem. J. 125 (2016) 1–9. doi:10.1016/j.microc.2015.10.040.

[14]   T. Rivas, S. Pozo, M.P. Fiorucci, A.J. López, A. Ramil, Nd:YVO4 laser removal of graffiti from granite. Influence of paint and rock properties on cleaning efficacy, Appl. Surf. Sci. 263 (2012) 563–572. doi:10.1016/j.apsusc.2012.09.110.

[15]   A. Costela, I. García-Moreno, C. Gómez, O. Caballero, R. Sastre, Cleaning graffitis on urban buildings by use of second and third harmonic wavelength of a Nd:YAG laser: A comparative study, Appl. Surf. Sci. 207 (2003) 86–99. doi:10.1016/S0169-4332(02)01241-2.

[16]   C. Gómez, A. Costela, I. García-Moreno, R. Sastre, Comparative study between IR and UV laser radiation applied to the removal of graffitis on urban buildings, Appl. Surf. Sci. 252 (2006) 2782–2793. doi:10.1016/j.apsusc.2005.04.051.

[17]   T. Learner, A review of synthetic binding media in twentieth-century paints, Conserv. 24 (2000) 96–103. doi:10.1080/01410096.2000.9995156.

[18]   V. Antúnez, P. Ortíz, J.-M. Martin, A. Gómez, R. Ortíz, Evaluación de Métodos de Limpieza de Graffiti en Mármol, Macla. 16 (2012) 68–69. doi:10.1002/col.20322.

[19]   P. Ortiz, V. Antúnez, R. Ortiz, J.M. Martín, M.A. Gómez, A.R. Hortal, B. Martínez-Haya, Comparative study of pulsed laser cleaning applied to weathered marble surfaces, Appl. Surf. Sci. 283 (2013) 193–201. doi:10.1016/j.apsusc.2013.06.081.

[20]   S. Samolik, M. Walczak, M. Plotek, A. Sarzynski, I. Pluska, J. Marczak, Investigation into the removal of graffiti on mineral supports: Comparison of nano-second Nd:YAG laser cleaning with traditional mechanical and chemical methods, Stud. Conserv. 60 (2015) 58–64. doi:10.1179/0039363015Z.000000000208.

[21]   M. Carvalhão, A. Dionísio, Evaluation of mechanical soft-abrasive blasting and chemical cleaning methods on alkyd-paint graffiti made on calcareous stones, J. Cult. Herit. 16 (2015) 579–590. doi:10.1016/j.culher.2014.10.004.

[22]   A. Dionísio, T. Ribeiro, When graffiti is not art: the damage of alkyd sprays on calcareous stones employed in cultural heritage, in: Cult. Herit., 2013: pp. 279–291.

[23]   F. Govaert, M. Bernard, Discriminating red spray paints by optical microscopy, Fourier transform infrared spectroscopy and X-ray fluorescence, Forensic Sci. Int. 140 (2004) 61–70. doi:10.1016/j.forsciint.2003.11.015.

[24]   V. Fassina, General criteria for the cleaning of stone: theoretical aspects and methodology of application, Stone Mater. Monum. Diagnosis Conserv. Sc. Univ. C.U.M. Conserv. Dei Monum. Heraklion, Crete, Mario Adda Ed. Bari. (1993) 126–132.

[25] R. Snethlage, K. Sterflinger, No Title, Stone Conserv. S. Durability, R. Siegesmund, Snethlage (Eds.), Stone Archit. Prop. Durability, Springer, Berlin Heidelb. (2011) 411–544.

[26] H.R. Sasse, R. Snethlage, Methods for evaluation of stone conservation treatments, N.S. Baer, R. Snethlage (Eds.), Dahlem Work. Rep. Sav. Our Archit. Herit. Conserv. Hist. Stone Struct. John Wiley Sons Ltd, West Sussex. 223–243 (1996).

[27] L. Lazarini, M.L. Tabasso, Il restauro della pietra, CEDAM-Casa Editrice Dott. A. Millani, Padova, 1986.

[28] E. Doehne, C.A. Price, Stone Conservation: An Overview of Current Research, 2nd edition, 2011. doi:10.1016/0006-3207(70)90031-5.

[29] A.E. Grimmer, Keeping it Clean : Removing Exterior Dirt, Paint, Stains and Graffiti from Historic Masonry Buildings, Library of Congress Cataloging-in-Publication Data, 1988. doi:10.1017/CBO9781107415324.004.

[30] S. Chapman, Laser technology for graffiti removal, J. Cult. Herit. 1 (2000) 75–78. doi:10.1016/S1296-2074(00)00153-9.

[31] N. Careddu, O. Akkoyun, An investigation on the efficiency of water-jet technology for graffiti cleaning, J. Cult. Herit. 19 (2016) 426–434. doi:10.1016/j.culher.2015.11.009.

[32] J.S. Pozo-Antonio, M.P. Fiorucci, T. Rivas, A.J. López, A. Ramil, D. Barral, Suitability of hyperspectral imaging technique to evaluate the effectiveness of the cleaning of a crustose lichen developed on granite, Appl. Phys. A Mater. Sci. Process. 122 (2016) 1–9. doi:10.1007/s00339-016-9634-5.

[33] C. Fotakis, D. Anglos, V. Zafiropoulos, S. Georgiou, V. Tornari, Lasers in the Preservation of Cultural Heritage: Principles and Applications, Taylor & Francis Group, London, 2006.

[34] P. Pouli, C. Fotakis, B. Hermosin, C. Saiz-Jimenez, C. Domingo, M. Oujja, M. Castillejo, The laser-induced discoloration of stonework; a comparative study on its origins and remedies, Spectrochim. Acta - Part A Mol. Biomol. Spectrosc. 71 (2008) 932–945. doi:10.1016/j.saa.2008.02.031.

[35] G. Daurelio, A Bronze Age pre-historic dolmen: laser cleaning techniques of paintings and graffiti (the Bisceglie Dolmen case study), in: Lasers Conserv. Artworks LACONA V Proceedings., Osnabrück, Germany., 2003: pp. 199–205.

[36] S.E. Andriani, I.M. Catalano, G. Daurelio, A. Albanese, Marker and pen graffiti cleaning on diverse calcareous stones by different laser techniques, in: Proc. SPIE 6346, XVI Int. Symp. Gas Flow, Chem. Lasers, High-Power Lasers., 2007: p. 634636–1/10. doi:10.1117/12.739334.

[37] R.. Esbert, C.. Grossi, a Rojo, F.. Alonso, M. Montoto, J. Ordaz, M.. Pérez de Andrés, C. Escudero, M. Barrera, E. Sebastián, C. Rodríguez-Navarro, K. Elert, Application limits of Q-switched Nd:YAG laser irradiation for stone cleaning based on colour measurements, J. Cult. Herit. 4 (2003) 50–55. doi:10.1016/S1296-2074(02)01227-X.

[38] C.M. Grossi, F.J. Alonso, R.M. Esbert, A. Rojo, Effect of laser cleaning on granite color, Color Res. Appl. 32 (2007) 152–159. doi:10.1002/col.20299.

[39] E. Urones-Garrote, A.J. López, A. Ramil, L.C. Otero-Díaz, Microstructural study of the origin of color in Rosa Porriño granite and laser cleaning effects, Appl. Phys. A Mater. Sci. Process. 104 (2011) 95–101. doi:10.1007/s00339-011-6344-x.

[40] A. Ramil, J.S. Pozo-Antonio, M.P. Fiorucci, A.J. López, T. Rivas, Detection of the optimal laser fluence ranges to clean graffiti on silicates, Constr. Build. Mater. 148 (2017) 122–130. doi:10.1016/j.conbuildmat.2017.05.035.

[41] S. Pozo, P. Barreiro, T. Rivas, P. González, M.P. Fiorucci, Effectiveness and harmful effects of removal sulphated black crust from granite using Nd:YAG nanosecond pulsed laser, Appl. Surf. Sci. 302 (2014) 309–313. doi:10.1016/j.apsusc.2013.10.129.

[42] S. Tambe, K.L. Gauri, S. Li, W.G. Cobourn, Kinetic study of sulfur dioxide reaction with dolomite, Environ. Sci. Technol. 25 (1991) 2071–2075. doi:10.1021/es00024a013.

[43] J.B. Johnson, S.J. Haneef, B.J. Hepburn, A.J. Hutchinson, G.E. Thompson, G.C. Wood, Laboratory exposure systems to simulate atmospheric degradation of building stone under dry and wet deposition conditions., Atmos. Environ. Part A, Gen. Top. 24A (1990) 2585–2592. doi:10.1016/0960-1686(90)90136-B.

[44] J. Simão, E. Ruiz-Agudo, C. Rodriguez-Navarro, Effects of particulate matter from gasoline and diesel vehicle exhaust emissions on silicate stones sulfation, Atmos. Environ. 40 (2006) 6905–6917. doi:10.1016/j.atmosenv.2006.06.016.

[45] C. Rodriguez-Navarro, E. Sebastian, Role of particulate matter from vehicle exhaust on porous building stones (limestone) sulfation, Sci. Total Environ. 187 (1996) 79–91. doi:10.1016/0048-9697(96)05124-8.

[46] P. Ausset, M. Del Monte, R.A. Lefèvre, Embryonic sulphated black crusts on carbonate rocks in atmospheric simulation chamber and in the field: Role of carbonaceous fly-ash, Atmos. Environ. 33 (1999) 1525–1534. doi:10.1016/S1352-2310(98)00399-9.

[47] B. Prieto, P. Sanmartín, B. Silva, F. Martínez-Verdú, Measuring the color of granite rocks: A proposed procedure, Color Res. Appl. 35 (2010) 368–375. doi:10.1002/col.20579.

[48] W. Mokrzycki, M. Tatol, Color difference Delta E-A survey, Mach. Graph. Vis. 20 (2011) 383–411.

[49] ISO 2409, Paints and varnishes — Cross-cut test, (2013).

[50] M. Masieri, M. Lettieri, Influence of the Distribution of a Spray Paint on the Efficacy of Anti-Graffiti Coatings on a Highly Porous Natural Stone Material, Coatings. 7 (2017) 18. doi:10.3390/coatings7020018.

[51] T.M. Tu, C.H. Chen, C.I. Chang, A posteriori least squares orthogonal subspace projection approach to desired signature extraction and detection, IEEE Trans. Geosci. Remote Sens. 35 (1997) 127–139. doi:10.1109/36.551941.

[52] P. Gaspar, C. Hubbard, D. McPhail, A. Cummings, A topographical assessment and comparison of conservation cleaning treatments, J. Cult. Herit. 4 (2003) 294–302. doi:10.1016/S1296-2074(02)01211-6.

[53] F.X. Perrin, M. Irigoyen, E. Aragon, J.L. Vernet, Artificial aging of acrylurethane and alkyd paints: A micro-ATR spectroscopic study, Polym. Degrad. Stab. 70 (2000) 469–475. doi:10.1016/S0141-3910(00)00143-9.

[54] G. Socrates, Infrared and Raman characteristic group frequencies, 2004. doi:10.1002/jrs.1238.

[55] A. Marrion, The Chemistry and Physics of Coatings, Second, 2004. doi:10.1017/CBO9781107415324.004.

[56] M.B. Smith, J. March, March's Advanced Organic Chemistry: Reactions, Mechanisms, and Structure: Sixth Edition, 2006. doi:10.1002/9780470084960.

[57] M.J.. Mosquera, T.. Rivas, B.. Prieto, B.. Silva, Capillary rise in granitic rocks: Interpretation of kinetics on the basis of pore structure, J. Colloid Interface Sci. 222 (2000) 41–45. doi:10.1006/jcis.1999.6612.

[58] IGME-Mapa Geológico de España E 1:50000, Hoja 261 Tui, Segunda Ed, 1981.

[59] V. Barrientos, J. Delgado, V. Navarro, R. Juncosa, I. Falcon, A. Vazquez, Characterization and geochemical-geotechnical properties of granite sawdust produced by the dimension stone industry of O Porrino (Pontevedra, Spain), Q. J. Eng. Geol. Hydrogeol. 43 (2010) 141–155. doi:10.1144/1470-9236/08-098.

[60] RILEM Recommandations provisoires, Essais recommandés pour mesurer l'altération des pièrres, Test n. II.1 Open Porosity, Commission 25 PEM, Prot. Eros. Des Monum. (1980).

[61] Levantina, Rosa Porriño granite - Tecnical file, (2017) 01–04. http://www.levantina.com/wp-content/uploads/2017/03/41-Rosa-Porri_o-Ficha.pdf (accessed September 12, 2017).

7. Appendix

Appendix 7.1 – Distribution of graffiti cleaning studies by stone type (A) and by graffiti removal methods (B)
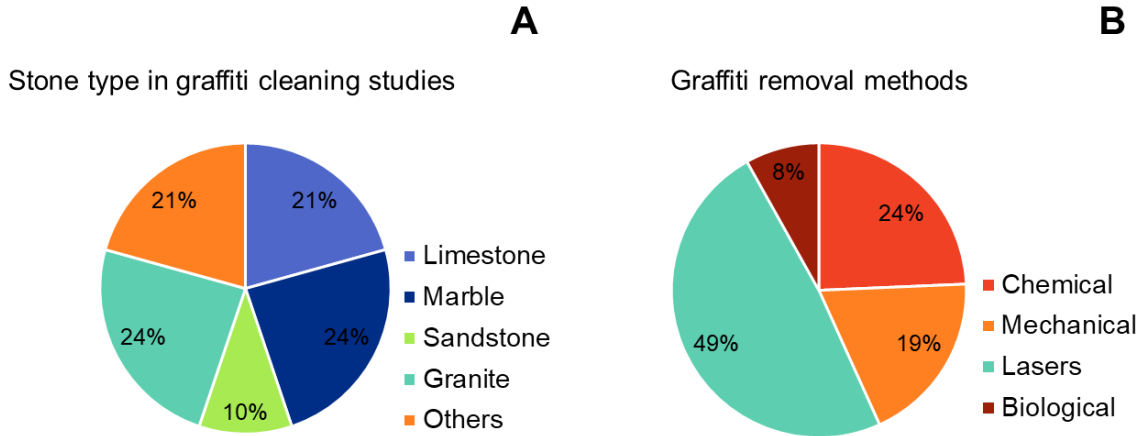
A **B**

Fig.7.1 - Distribution of graffiti cleaning studies by stone type (A) limestone, marble, sandstone, granite and others and by graffiti removal methods (B) chemical, mechanical, laser and biological.

Appendix 7.2 – Brief petrographic description and technical specifications of Rosa Porriño granite

Rosa Porriño it is a two-mica calcoalkaline coarse-grained granite with a panallotriomorphic heterogranular texture composed of 40% quartz (grain sizes from 3.8-0.8 mm), 27% potassium feldspar (microcline, grain sizes reaching 10 mm), 14% plagioclase (grain sizes smaller than 1.8 mm), 8% biotite (1-2 mm in grain size), 2% muscovite and 5% accessory minerals [58]. The major element chemical composition (in wt%) is 71.9% SiO_2, 13.7% Al_2O_3, 2.55 Fe_2O_3, 0.94% CaO, 6.94% K_2O, 3.34% Na_2O, 0.25% MgO, 0.05% P_2O_5, 0.025% MnO [59]. Open porosity is 0.85% [60].

Table 7.1 - Characteristics and physical-mechanical properties of Rosa Porriño granite [61].

Photograph	Characteristics	Value
	Petrographic denomination	Biotite granite
	Apparent density	2.612 (Kg/m3)
	Open porosity	0,70 (%)
	Water absorption by atmospheric pressure	0,3 (%)
	Compression resistance	103 ± 28,3 (MPa)
	Flexural strength under concentrated load	9,7 ± 1,2 (MPa)
	Decreasing of flexural strength after 48 cycles frost-taw	< 0,02 (%)
	Abrasion resistance	17,0 ± 0,2 (mm)

Appendix 7.3 – Technical data sheets of the used abrasives

The technical data sheets were provided by ClinArte S.L. company. The brand of the abrasives is unknown since it is considered by the company confidential information.

Silicon

Composition: $SiO_2 \approx 98.6$ %, $Al_2O_3 \approx 0.800$ %, $TiO_2 \approx 0.070$ %, $Fe_2O_3 \approx 0.050$ %, $K_2O \approx$ 0.400 % and $CaO \approx 0.030$%.

Size range: 106-75 µm (89.8%), 150-106 µm (6.9%), 212-150 µm (0.7%), 300-212 µm (0.2%). 425-300 µm (0.1%).

Hardness: 7 Mohs.

Density: 2.64 g/cm^3.

Aluminium silicate

Composition: $SiO_2 \approx 45$-52 %, $Al_2O_3 \approx 24$-31 %, $Fe_2O_3 \approx 7$-11 %, $CaO \approx 3$-8 %, $K_2O \approx$ 2-5 %, $MgO \approx 2$-3 %, $TiO \approx 0$-2 % and $Na_2O \approx 0$-1 %.

Size range: 160-80 µm.

Hardness: 7 Mohs.

Density: 2.4- 2.6 g/cm^3.

Calcium carbonate

Composition: $CaCO_3$ (~98%), CaF_2 (<0.5%), $Ca(NO_3)_2$ (<0.5%), NH_4NO_3 (<0.5%) and $Ca_3(PO_4)_2$ (<0.5%).

Size range: 70–200 µm.

Density: 2.83 g/cm^3

Appendix 7.4 – SEM micrographs of the tested abrasives
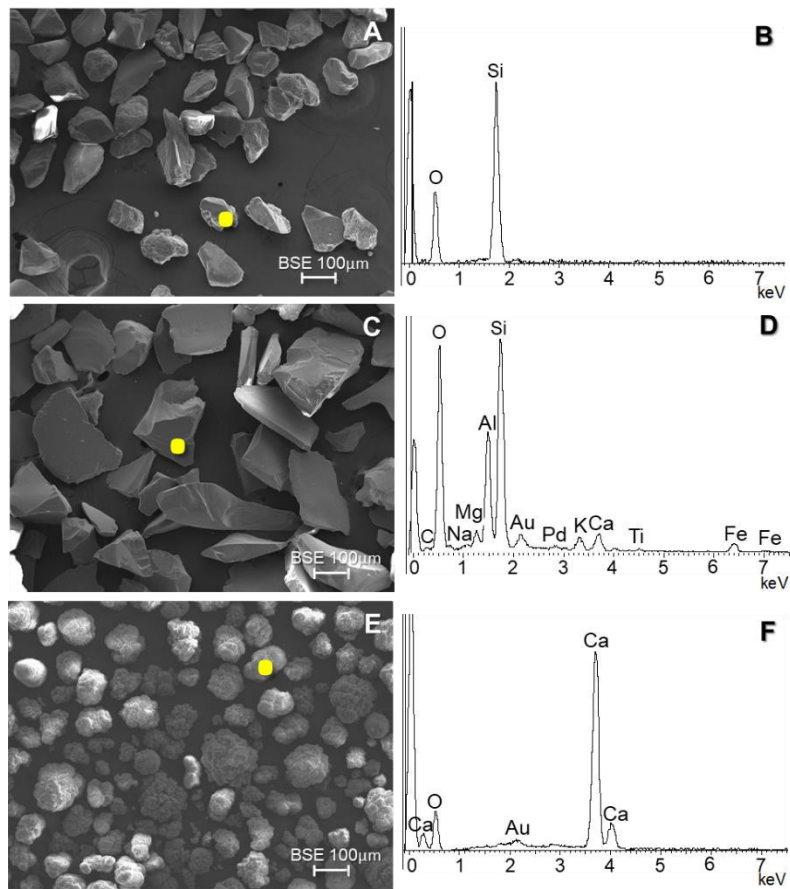
Fig.7.2 – SEM (BSE mode) of the abrasives with the respective EDS: silicon (A and B); aluminium silicate (C and D) and calcium carbonate (E and F).

Appendix 7.5 – Characteristics of the used laser

A Nd:YVO$_4$ Coherent AVIA Ultra 355–2000® laser at the 355 nm wavelength and with 25 ns pulse duration. The pulse repetition rate can be selected from a single-shot to 100kHz with around 0.1 mJ energy per pulse. A Galilean beam expander was arranged, to improve the focalization, with a 150 mm convergent lens, a diameter of D $\approx$ 150 μm and a fluence of 1.2 J.cm^{-2}. The target surface was placed on a motorized XYZ translation stage, with the Z axis of the impinged beam perpendicular to the sample surface. The beam scanning along parallel lines in X direction allowed a homogeneous irradiation of the target surface. The frequency (10 000 Hz), fluence (0.1-0.3 J.cm^{-2}), scan speed (25 mm.s^{-1}), distance between scans (0.075 mm) and laser trajectory parameters (horizontally and vertically alternated with no more than four scans) were selected on the basis of previous studies in granites [11–14,40]. Preliminary cleaning tests evaluated under stereomicroscope.

Appendix 7.6 – Analytical methods used: characteristics and conditions

XRF: ArtTAX, 800 spectrometer is equipped with an air-cooled low-power X-ray tube with a Mo target. The primary X-ray beam is focused to a diameter of 70 mm by means of polycapillary X-ray mini lens. In all cases the spectrometer was operated at 40 kV, 0.6 mA and 200 s acquisition time, in air atmosphere. The obtained data was treated with PANalytical software.

XRD: XPERT-PRO diffractometer with CuKα radiation at 40 kV and 30 mA, with a 2 theta step size of 0.1° and a counting time of 50.0313 s. The diffractometer is provided with automatic divergence slit.

Raman: LabRam HR Evolution spectrometer is equipped with a solid-state laser operating at 532 nm with a resolution of 6 cm^{-1} for the 600 grooves.mm^{-1} grating. The laser beam was focused with 100× Olympus objective lens. The samples were analyzed with 10 s laser exposure time for 16 scans and the data obtained was treated with Labspec software.

FTIR: Nicolet 6700 spectrometer with a DTGS KBr detector. The spectra were obtained in a transmission mode, between 400 and 4000 cm^{-1}, with a resolution of 4 cm^{-1} and 20 sample scans.

Spectrophotometer: The measurements were made in specular component included (SCI) mode, for a spot diameter of 8 mm with diffuse illumination by means of xenon flash arc lamp and 10 nm diffuse bandwidth, using illuminant D65 at observer angle 2°.

Hyperspectral: CCD sensor Pulnix TM-1327 GE with an objective lens, focal 10 mm and a spectrograph ImSpector V10 with 4.55 nm resolution, records a linear array of 1392 pixels of the object under analysis to obtain an image at each wavelength (1040) in the range of 400–700 nm.

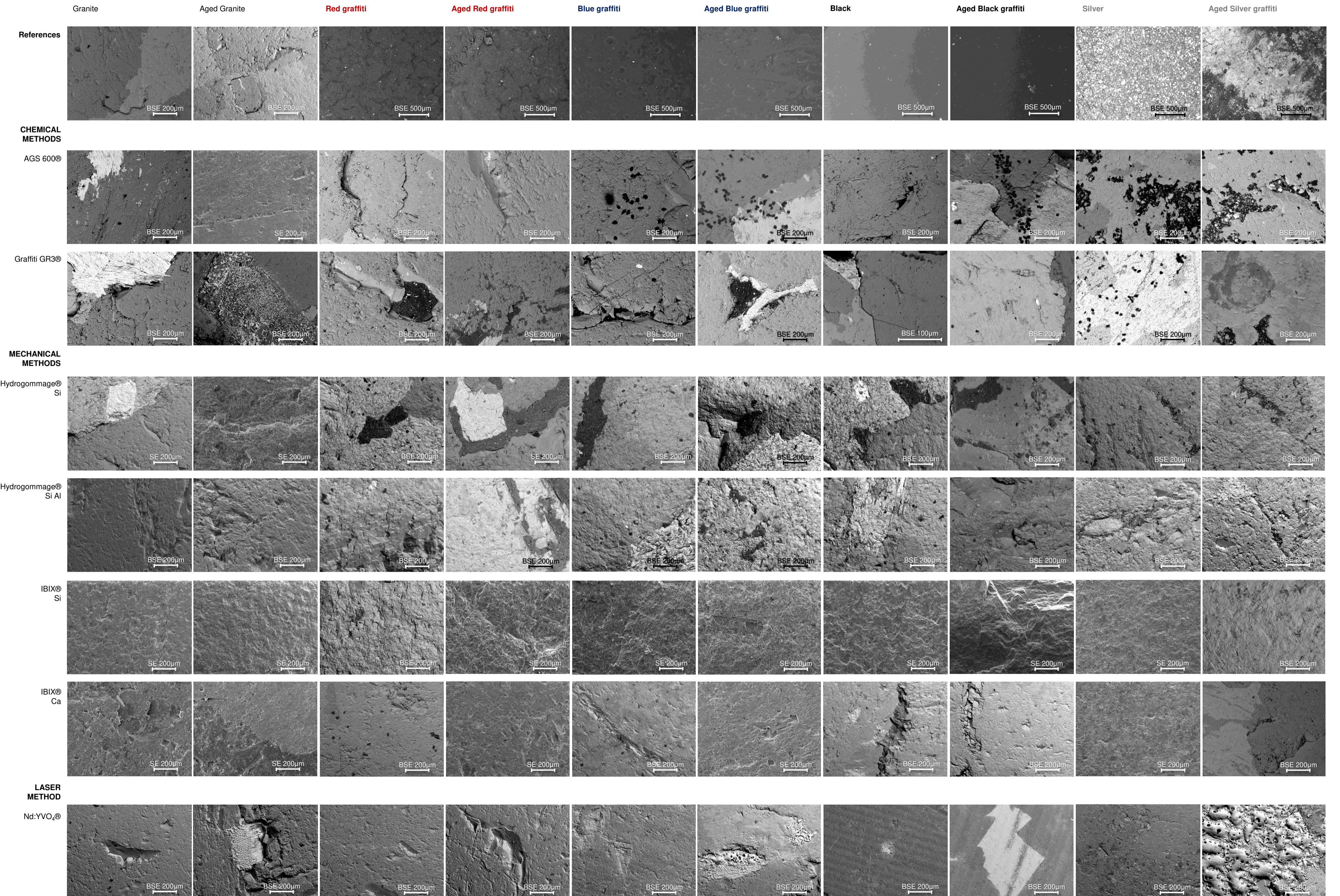# Appendix 7.7 – XRD aerosol graffiti paints peak list

Table 7.2 – XRD peak list of the three more intense peaks for each identified aerosol paint compound.

Compound Name	Chemical Formula	Ref. Code	Paints	d-spacing [Å]	Relative Intensity [%]
Aluminium	Al	00-004-0787	Unaged Silver	2.33712	100.00
				2.33712	50.00
				2.02414	45.60
			Aged Silver	2.34122	64.31
				2.02738	29.97
				1.22178	14.13
Titania	TiO_2	00-021-1276	Unaged Red	1.68396	100.00
				3.24581	71.71
				1.35728	50.08
			Aged Red	3.24786	100.00
				1.68860	69.98
				2.48741	46.70
			Unaged Blue	3.25132	100.00
				1.68579	78.48
				2.48760	54.37
			Aged Blue	3.24661	100.00
				1.68758	68.16
				2.48676	52.35
Barite	$BaSO_4$	00-024-1035	Aged Red	2.48741	46.70
				1.36109	27.21
				1.34756	13.40
Gypsum	$CaSO_4 \cdot 2H_2O$	00-006-0046	Aged Red	1.68860	69.98
				2.48741	46.70
				1.62504	22.47
			Aged Black	4.26382	100.00
				3.06051	65.75
				2.86627	52.53
Graphite	C	00-025-0284	Aged Black	3.34218	77.87
Alunogen	$Al_2(SO_4)_3 \cdot 16H_2O$	00-016-0360	Aged Silver	4.49987	100.00
				13.59022	24.53
				2.96491	5.86
Metalunogen	$Al_2(SO_4)_3 \cdot 12H_2O$	00-021-0011	Aged Silver	2.02738	29.97
				3.02874	14.89
				1.92344	2.41

Appendix 7.8 – Number of cleaner applications, number of passages and necessary time to achieve a satisfactory cleaning level for chemical, mechanical and laser methods

Table 7.3 – Number of cleaner applications (ap) for chemical methods (*AGS* and *GR3*); number of passages (p) for laser (*Nd:YVO₄*) and necessary time (t) referred in seconds for mechanical methods (*Hydro* and *IBIX*) , to achieve a satisfactory cleaning level. The prefix A marks the samples that were subjected to ageing before the respective cleaning procedure.

Cleaning methods	Granite	Red paints	Blue paints	Black paints	Silver paints
AGS	4 (p)	4 (p)	4 (p)	4 (p)	4 (p)
A-AGS	5 (p)	5 (p)	5 (p)	5 (p)	5 (p)
GR3	1 (p)	4 (p)	2 (p)	1 (p)	1 (p)
A-*GR3*	3 (p)	5 (p)	4 (p)	5 (p)	3 (p)
*Hydro S*i	0.10 s (t)	0.10 s (t)	0.10 s (t)	0.10 s (t)	0.10 s (t)
A-*Hydro Si*	0.20 s (t)	0.20 s (t)	0.20 s (t)	0.20 s (t)	0.20 s (t)
Hydro Si Al	0.05 s (t)	0.05 s (t)	0.05 s (t)	0.05 s (t)	0.05 s (t)
A-*Hydro Si Al*	0.10 s (t)	0.10 s (t)	0.10 s (t)	0.10 s (t)	0.10 s (t)
IBIX Si	0.05 s (t)	0.05 s (t)	0.05 s (t)	0.05 s (t)	0.05 s (t)
A-*IBIX Si*	0.10 s (t)	0.10 s (t)	0.10 s (t)	0.10 s (t)	0.10 s (t)
IBIX Ca	0.05 s (t)	0.05 s (t)	0.05 s (t)	0.05 s (t)	0.05 s (t)
A-*IBIX Ca*	0.10 s (t)	0.10 s (t)	0.10 s (t)	0.10 s (t)	0.10 s (t)
Nd:YVO₄	2 (p)	2 (p)	3 (p)	3 (p)	4 (p)
A-*Nd:YVO₄*	2 (p)	2 (p)	3 (p)	3 (p)	4 (p)

Appendix 7.9 – SEM micrographs of aged and unaged stone, graffiti aerosol paints and cleaned surfaces

	Granite	Aged Granite	Red graffiti	Aged Red graffiti	Blue graffiti	Aged Blue graffiti	Black	Aged Black graffiti	Silver	Aged Silver graffiti
References										
CHEMICAL METHODS										
AGS 600®										
Graffiti GR3®										
MECHANICAL METHODS										
Hydrogommage® Si										
Hydrogommage® Si Al										
IBIX® Si										
IBIX® Ca										
LASER METHOD										
Nd:YVO₄®										

Appendix 7.10 – Colorimetric data of aged and unaged stone, graffiti aerosol paints and cleaned surfaces

Table 7.4 - L*, a*, b* average data obtained for the stone, paint and cleaned surfaces with and without SO_2 ageing. The prefix A marks the samples that were subjected to ageing before the respective cleaning procedure.

Cleaning methods	Granite			Red paints			Blue paints			Black paints			Silver paints		
	L*	a*	b*	L*	a*	b*	L*	a*	b*	L*	a*	b*	L*	a*	b*
Reference	66.51	3.86	6.91	44.25	43.27	16.90	37.82	1.31	26.14	31.17	0.01	0.20	88.45	0.45	0.64
A-Reference	72.66	2.85	10.34	46.90	37.74	13.66	38.37	0.27	20.58	30.15	0.09	0.06	54.11	0.68	0.69
AGS	64.46	3.45	7.87	68.51	5.10	9.61	63.11	2.00	5.73	61.76	4.96	9.34	60.26	2.86	6.66
A-AGS	62.88	2.95	8.21	57.22	5.99	8.17	62.35	2.11	5.92	59.51	2.67	6.34	48.25	1.88	5.11
GR3	61.61	2.23	5.68	65.31	6.70	11.28	61.52	3.12	6.49	58.73	2.61	6.13	64.49	5.19	9.80
A-GR3	61.68	3.00	7.43	55.60	3.82	7.40	56.25	0.53	1.85	56.04	2.91	7.07	62.45	1.71	6.50
Hydro Si	68.58	4.56	7.43	65.32	4.26	7.43	62.47	3.69	6.49	60.69	2.91	6.38	66.58	4.20	8.17
A-Hydro Si	68.50	5.87	9.38	65.52	3.83	7.42	63.94	3.63	6.66	64.33	3.26	6.26	63.37	4.31	7.97
Hydro Si Al	69.28	4.48	7.93	66.71	5.08	9.49	63.49	2.75	6.29	58.37	2.22	5.32	61.28	4.33	8.01
A-Hydro Si Al	67.98	4.80	9.67	65.38	4.24	7.36	61.95	2.55	5.50	64.55	3.02	6.22	63.06	5.03	8.83
IBIX Si	65.71	3.02	6.98	65.21	3.31	5.79	66.13	2.85	5.54	65.65	3.63	6.38	63.85	3.17	5.97
A-IBIX Si	69.55	4.19	6.98	65.54	3.29	6.13	67.01	3.98	6.71	66.76	3.62	6.76	65.57	3.09	6.04
IBIX Ca	65.71	3.44	6.53	61.70	4.27	6.74	62.95	3.17	6.33	60.24	3.09	5.83	64.11	6.45	10.90
A-IBIX Ca	63.12	4.54	9.74	63.36	7.73	11.88	61.59	2.50	5.46	60.98	5.17	9.48	57.16	3.93	7.37
Nd:YVO$_4$	66.28	1.99	4.98	56.63	3.38	8.14	54.95	0.00	4.63	56.17	2.05	9.76	58.40	1.74	5.85
A-Nd:YVO$_4$	68.00	3.43	8.76	48.11	2.95	5.81	51.27	1.62	2.52	59.37	2.62	9.19	51.79	2.45	7.22

Appendix 7.11 – Surface roughness average and standard deviation data (Ra) of aged and unaged stone, graffiti aerosol paints and cleaned surfaces

Table 7.5 – Surface roughness average - Ra (µm). The prefix A marks the samples that were subjected to ageing before the respective cleaning procedure. *1 There are significant differences between the reference and after the cleanings to reject the null hypothesis with a confidence interval of 95%, *2 Roughness damage attributed to the cleaning performance.

Cleaning methods	Granite [µm]	Red paints [µm]	Blue paints [µm]	Black paints [µm]	Silver paints [µm]
Reference	1.925 ± 0.929	0.735 ± 0.322*1	0.465 ± 0.128*1	1.291 ± 1.225	2.635 ± 1.182
A-Reference	1.721 ± 1.387	0.899 ± 0.586*1	0.553 ± 0.301*1	0.656 ± 0.331*1	10.646 ± 3.367*1
AGS	1.829 ± 1.096	1.635 ± 1.442	1.130 ± 0.374 *1	1.907 ± 1.353	2.069 ± 1.205
A-AGS	1.900 ± 0.464	2.302 ±1.401	1.407 ± 0.556	2.195 ± 0.872	2.153 ± 2.043
GR3	1.724 ± 1.308	1.348 ±0.535	1.850 ± 1.140	1.869 ± 2.155	2.018 ± 0.873
A-GR3	1.655 ± 0.858	1.410 ±0.661	1.116 ± 0.509 *1	2.076 ± 1.599	1.802 ± 0.875
Hydro Si	3.359 ± 1.022 *1, 2	3.868 ± 0.756 *1, 2	3.784 ± 0.521 *1, 2	3.922 ± 0.954 *1, 2	3.724 ± 2.005 *1, 2
A-Hydro Si	3.943 ± 1.732 *1, 2	4.300 ± 1.218 *1, 2	4.344 ± 1.395 *1, 2	4.596 ± 0.947 *1, 2	3.236 ± 0.970 *1, 2
Hydro Si Al	4.135 ± 1.649 *1, 2	4.147 ± 1.150 *1, 2	4.270 ± 0.687 *1, 2	4.678 ± 1.378 *1, 2	4.526 ± 1.400 *1, 2
A-Hydro Si Al	3.956 ± 1.833 *1, 2	4.111 ± 0.985 *1, 2	3.764 ± 1.462 *1, 2	3.910 ± 0.710 *1, 2	3.399 ± 0.814 *1, 2
IBIX Si	4.555 ± 1.437 *1, 2	6.443 ± 1.210 *1, 2	5.796 ± 1.672 *1, 2	6.716 ± 1.740 *1, 2	6.387 ± 1.405 *1, 2
A-IBIX Si	5.868 ± 1.945 *1, 2	7.101 ± 1.917 *1, 2	5.605 ± 1.408 *1, 2	5.540 ± 0.924 *1, 2	5.311 ± 2.717 *1, 2
IBIX Ca	4.464 ± 2.308 *1, 2	3.165 ± 2.231 *2	1.863 ± 0.928	2.860 ± 1.188 *2	2.310 ± 1.413
A-IBIX Ca	3.302 ± 1.773 *2	1.691 ±0.859	2.849 ± 1.118	1.678 ± 1.208	2.804 ± 1.433
Nd:YVO$_4$	1.411 ± 0.734	1.251 ± 0.969	0.836 ± 0.296 *1, 2	1.588 ± 0.964	2.261 ± 1.504
A-Nd:YVO$_4$	4.092 ± 2.184 *1, 2	1.680 ± 0.868	1.770 ± 0.884	2.041 ± 1.790	1.736 ± 0.955

Table 7.6 – Average static contact angle measurements represented in intervals of minimum (Min.), maximum (Max.) and average (Ave.) The prefix A marks the samples that were subjected to ageing before the respective cleaning procedure.

Cleaning methods	Granite			Red paints			Blue paints			Black paints			Silver paints		
	Min.	Max.	Ave.	Min.	Max.	Ave.	Min.	Max.	Ave.	Min.	Max.	Ave.	Min.	Max.	Ave.
Reference	52.76	40.28	44.80	84.90	77.70	81.94	89.56	80.01	84.80	91.88	72.96	85.27	98.87	82.94	90.65
A-Reference	100.91	53.75	70.87	82.62	58.60	72.13	80.52	70.36	76.17	84.48	69.57	79.04	74.38	51.91	65.48
AGS	48.53	36.92	43.21	73.19	67.68	69.42	63.74	49.66	58.37	62.57	46.12	54.89	102.72	83.07	94.38
A-AGS	54.66	28.00	40.76	86.60	69.43	77.96	72.90	63.02	66.08	86.14	59.38	72.91	118.48	91.20	99.43
GR3	52.99	44.45	48.77	79.49	46.52	65.01	90.45	69.11	82.32	76.55	43.79	60.29	106.48	82.19	98.86
A-GR3	75.63	66.40	72.15	89.70	80.00	86.44	93.30	75.68	82.72	84.71	63.89	75.38	112.64	92.33	99.57
Hydro Si	58.98	29.00	46.19	66.47	41.48	56.42	63.00	55.80	58.48	52.60	41.78	48.45	72.70	65.88	68.89
A-Hydro Si	77.93	51.61	68.27	87.34	72.67	77.11	88.42	65.68	82.14	86.15	68.17	80.12	109.33	83.41	96.27
Hydro Si Al	78.71	44.95	61.91	73.33	51.63	59.84	69.13	62.81	65.72	97.90	79.14	89.51	77.85	48.37	68.53
A-Hydro Si Al	94.92	59.59	82.72	100.95	86.10	94.18	99.93	88.78	94.77	111.17	80.67	93.39	111.19	87.09	98.04
IBIX Si	49.48	28.17	38.36	40.62	24.64	32.90	52.54	24.79	39.06	98.57	64.79	87.34	67.09	42.79	57.45
A-IBIX Si	92.80	34.20	64.05	95.27	59.93	79.76	84.40	70.13	78.19	127.30	50.51	94.23	104.45	94.77	99.41
IBIX Ca	52.13	45.53	48.85	77.59	56.42	67.70	93.43	67.52	81.69	85.12	59.20	71.29	95.63	49.83	73.41
A-IBIX Ca	85.71	64.93	72.47	106.57	76.85	89.33	113.49	51.28	86.61	104.00	73.46	86.01	117.11	99.63	108.96
Nd:YVO$_4$	79.55	58.06	67.88	79.99	71.46	75.51	87.37	74.59	82.27	78.84	66.49	72.42	89.38	68.89	80.80
A-Nd:YVO$_4$	96.00	78.76	89.01	83.18	75.00	79.20	102.20	85.02	91.04	84.32	71.94	77.50	96.85	85.63	90.20